STUDY OF CERAMIC/METAL INTERFACE STRUCTURE

By

Indrani Chakravarty

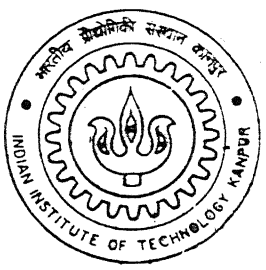

DEPARTMENT OF MATERIALS AND METALLURGICAL ENGINEERING

Indian Institute of Technology Kanpur

APRIL, 2002

STUDY OF CERAMIC/METAL INTERFACE STRUCTURE

A Thesis Submitted
In Partial Fulfilment Of The Requirements
For The Degree Of

MASTER OF TECHNOLOGY

by

INDRANI CHAKRAVARTY

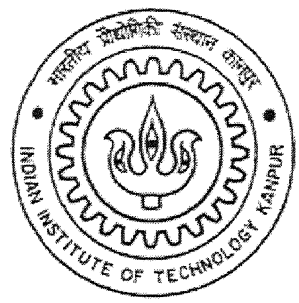

to the

DEPARTMENT OF MATERIALS AND METALLURGICAL ENGINEERING

INDIAN INSTITUTE OF TECHNOLOGY, KANPUR

APRIL, 2002

CERTIFICATE

This is to certify that the work contained in the thesis entitled "*Study of ceramic/metal interface structure*" by Indrani Chakravarty has been carried out under my guidance and that this work has not been submitted elsewhere for a degree.

Dr. S.P.Gupta

Professor
Department of Materials and Metallurgical Engineering,
Indian Institute of Technology, Kanpur

ACKNOWLEDGEMENT

I take this opportunity to express my sincere thanks and profound sense of gratitude to my guide, Prof. S.P. Gupta, for his guidance, inspiration and encouragement during the course of this project. He has taught me the values of research and independent thinking. He spent tremendous time and effort on me and was always ready to help and discuss my difficulties.

I would also like to thank all the laboratory staff members of Deptt. Of MME, IIT Kanpur, who directly or indirectly extended their co-operation for completion of this work. I also take the opportunity to thank my friends, Aditya, Suresh Babu, Madhuri, Satish, Amit, Sankaran, Sudhir and others.

I wish to express my sincere indebtedness to my husband, our parents and my sisters, whose deep affection and silent inspiration have always guided me towards success.

Indrani Chakravarty

Abstract:

Ceramics to metals can be joined effectively in a number of ways. By far th simplest method is to use an activated brazing alloy. It cuts out severa processing steps when compared with the Moly-Manganese Metallisin process, and if careful preparation of the ceramic is maintained, results can b just as successful. Alumina, silicon carbide, silicon nitride, graphite, diamon and many other engineering materials can be successfully brazed using activ braze alloys. More filler metals, which can operate above 1050^0C, ar increasingly being sought after to join hot engine components.

In this work, attempt has been made to study the formation and growth c intermetallic compounds in the ceramic to metal systems, produced by activ brazing process. In this process alumina has been used as the ceramic membe and Fe, Ni, Nb, Ta etc were used as the metal members, and 60Ag-30Cu-10S the filler metal and pure Ti as the active metal. The process was carried out a 800^0C for a holding time of 16 hours for each specimen under vacuum of 10 Torr and cooled first in vacuum and then in air.

A number of binary and ternary compounds have been observed to form the metal-filler metal, filler metal-active metal and active metal-ceram interfaces. While a part of the filler metal remain unchanged, a number intermetallic compounds for example TiCu, TiFe, $TiCu_2$, $TiFe_2$ etc analyz using electron probe micro analyzer (EPMA). The composition of t intermetallic compounds has been analyzed. The possible substitution of one more of the components of the intermetallic compounds by Cu, Ag, Sn, Ti, and the refractory metals has been analyzed.

Contents:

Page No.

List of Tables:

List of Figure:

1. INTRODUCTION:

The ability to produce reliable brazed ceramic/metal joints is a key enabling technology for many production, prototype and advanced developmental items and assemblies. The application of ceramic in structural components such as turbine engines has received extensive attention in recent decades due to their excellent high temperature strength and resistance to corrosion and wear. However, ceramics possessing a brittle nature often face problem in several joining techniques. If properties of ceramics such as being more refractory and less dense than metals and at the same time being stronger are to be exploited then adequate joining technology is quite essential and that technology is brazing [1-7].

The American Welding Society defines brazing as **" a group of welding processes, which produces coalescence of materials by heating them to a suitable temperature and by using a filler metal having a liquidus temperature above 450°C and below the solidus temperature of the base materials. The filler metal is distributed between the closely fitted surfaces of the joint by capillary action."** The formation of strong bonds between materials of widely differing compositions and properties such as ceramics and metals is what we often get from brazing. Brazing can make joints that are accessible and parts that may not be joinable at all by other methods. Assemblies that are complicated due to shape, metal characteristics, and thickness can be turned into an integral component by brazing.

Ceramics are becoming increasingly important in engineering applications because of their excellent heat resistance, corrosion resistance; wear resistance, high temperature strength and stability, etc. On the other hand,

they have weaknesses in ductility, workability, mass production compared to metals. Recently, various efforts have been made to join ceramic-to-ceramic or ceramic to metal for electronic and structural applications such as diesel engine parts, turbines and heat exchangers.

1.1(a) Brazing: Brazing is often the preferred method for joining ceramics to metals because it can provide hermetic seals and the plasticity of the braze accommodate the differential expansion between the ceramic and metal. But several important problems such as the poor wettability, residual stresses due to thermal expansion mismatch between ceramics and metals still remain unsolved. Generally, ceramics have covalent or ionic bonding, but metals have metallic bonding in terms of atomic structures concerned w`ith free electrons. Thus, the creation of a metal/ceramic interface causes an electron discontinuity and can require more energy than the formation of a ceramic surface and hence result in poor wettability. Also, the coefficients of thermal expansion (CTE) of ceramics are usually smaller than that of metals, hence residual stresses generated after brazing process may cause significant tensile or compressive stresses on the ceramics or metals.

Next generation braze assembly designs have been simplified, in part, through the use of active metal brazing. The joining process eliminates ceramics metallization and related processing steps. The fundamental interfacial reactions that occur between the active constituents in the filler metal and alumina ceramics are not well understood, particularly for vanadium and zirconium-containing alloy systems. A more science-based approach to understanding, predicting controlling, and optimizing these reactions is required before active brazing can see widespread application. Brazing has many advantages over welding and in most cases; the cost is

very competitive with welding. The advantages of brazing include cosmetic appearance, cleanliness, and baked-out surfaces. The bonding of ceramics can be classified into 3 areas depending on their temperature of usage. (a) Low Temperature - below 500C, (b) Intermediate temperature - between 500 and 1050C, (c) High Temperature - above 1050C.

Intermediate temperature usage: This range of temperature is between 500 and 1050C. The most commonly used Ceramic in this range is Alumina, and grades of alumina vary from 94% upwards. For temperatures below 1050C, there are two main brazing methods of joining Ceramics to Metals. Firstly we have metallization that is by applying coating that promote wetting to the ceramic surface prior to brazing & secondly we have brazing with standard braze alloys with some active metals that activate wetting and ceramic can be brazed directly [ABA].

1.1(b) Active Brazing: In Active Brazing, the ceramic and metal components are brazed directly onto the surface of the component using an active braze alloy [ABA]. ABA's contain elements such as titanium or vanadium which react chemically with the ceramic component, and enhance the wetting ability of the braze alloy onto the ceramic.

The process mechanism that enables the ABA to wet the ceramic is a chemical reaction between the active element (Ti or V etc.) in the braze alloy with the ceramic. The exact reaction products, however, are not so well understood. In all cases reported, the reaction products with titanium are many and varied, with many complex reactions taking place in the same series of experiment

The brazing filler metal has several requirements in active brazing. It should be able to wet the ceramic and for a fillet for inspection purposes. It should also be ductile enough to plastically deform during cooling in order

Literature on Active Brazing of Ceramics

Investigators	Year	Ceramic Substrate	Active Braze Alloy
Valentine, Nicholus & Waite (35)	1980	Al_2O_3	Cu-8Ti
Nicholus (36)	1989	Al_2O_3	Ag-2Cu-2Ti
Xian, Si, Zhou Shen & Li (37)	1991	Al_2O_3	Ag-28Cu-5Al-5Ti
Loehman, Tomsia, Pask & Johnson (38)	1990	Si_3N_4	Ag-Cu-Ti
Peteves, Paulastro, Ceccone & Stamos (39)	1998	Si_3N_4	Au-36Ni-5V-1Mo
Tillman, Lugscheider, Schlumbach, Manter & Indacochea (40)	1998	Si_3N_4	Ag-Cu-Ti, Pd-Ni-Ti, Pd-Cu-Ti, Pd-Cu-Pt-Ti
Timley, Huddleston & Lacey (41)	1998	SIALON	Ag-Cu-Ti
Santella & Pak (42)	1993	ZrO_2	Ti coating
Hao, Wang, Jin & Wang (43)	1995	ZrO_2	$Ag_{57}Cu_{38}Ti_5$
Yano & Suematsa	1988	SiC	Ag-Cu-Ti
Lee & Lee (44)	1992	SiC	Cu-Ti
Iwamoto & Tanaka (45)	1998	SiC	Ag-Cu-Ti

Table: 1

to accommodate the stresses, which are induced by different thermal expansion coefficients, that inevitably occur when a metal is joined to a ceramic. This leads to the dilemma of the braze alloy strength versus braze alloy ductility. In general, the higher the actual braze alloy strength, the higher the yield point, and therefore, the higher the residual stresses in the joint, which can lead to premature failure. This leads to the conclusion that for an effective ceramic to metal braze, it is not always the strongest braze alloy that is the best for that particular application.

Metal Component - Plastic deformation of the metal during cooling can accommodate the stresses incurred due to mismatch of thermal expansions. Low expansion metals such as molybdenum, while reducing the extent of the mismatch, are relatively brittle compared with copper or nickel, and may not be the best choice of material. Annealing the metal prior to brazing is always advisable if any work has been carried out such as pressing, forming or welding.

Brazing Temperature-There are two opposing factors in determining the maximum brazing temperature. The higher the temperature of brazing, the more active the ABA, and therefore, the better the wettability. Conversely, the higher the temperature, the more alloying occurs with the metal member, and the braze alloy has a lower viscosity. In very general terms, a temperature between 25-50 ^{0}C above the braze alloy liquidus nearly always gives good results.

1.1(c) Ceramics-Al_2O_3-applications-charecteristics, which create problem in brazing to metals: Ceramics are inorganic nonmetallic materials, separated into two broad categories (a) Traditional ceramics, which include clay products and refractotories. (b) Structural ceramic which include monolithic materials like Al_2O_3, ZrO_2, SiC, AlN, Si_3N_4 etc are in a

great technological interest due to their unique properties when compared to metals, such as maintaining high strength even at high temperature, excellent wear resistance, high hardness, excellent corrosion and oxidation resistance, low thermal expansion, and high electrical resistivity. Structural ceramics are being used or considered for use as cutting tools, bearings, machine-tool parts, dies, pump seals, high temperature heat exchangers and a variety of internal combustion and turbine engine parts. Largest fraction of ceramic is actually being used in the electronics industry and in the new and unusual engineering applications.

Al_2O_3 is still the most widely used structural ceramic with a sizeable commercial market, and in United States its application is dominated by the electronics field. These applications generally require an insulating material with some or all of the following properties: high mechanical strength for rectifier housings, high volume resistivity, low dielectric losses for transmitter tubes, high translucency for sodium vapor discharge lamps. Most of these requirements can be met only by high-purity structural grade of Al_2O_3.There are numerous specialty electronic applications for Al_2O_3, including spark plugs, high voltage insulators, vacuum-tube envelopes, rf windows, and integrated circuit packages. In all the above applications, braze joints hold a very integral role.

Generally, ceramics have covalent or ionic bonding, but metals have metallic bonding in terms of atomic structures concerned with free electrons. Thus, the creation of a metal/ceramic interface causes an electron discontinuity and can require more energy than the formation of a ceramic surface and hence result in poor wettability. Also, the coefficients of thermal expansion (CTE) of ceramics are usually smaller than that of metals, hence residual stresses generated after brazing process may cause significant

tensile or compressive stresses on the ceramics or metals. The above listed difference in properties of ceramic and metal are being taken into account in research work carried out.

1.2 Key parameters of brazing:

While describing the formation of brazed joints, two basic phenomena are to be described: (a) Wetting, (b) Flow of a liquid on the surface of a solid.

Wetting: Wetting of the base materials by the filler metal is required to provide intimate contact between them and to develop the bonding needed. The driving forces for these phenomena are characterized through the thermodynamic concepts of surface free energy, and the free energy of formation of phases which may result from chemical reaction that occur during brazement. Wettability is an important criteria for selection of filler metals and alloys that we will see in later sections.

Surface free energy: "The surface free energy of a solid or liquid is the excess free energy introduced by the presence of a surface" or in terms of a simple bonding concept for condensed phases "the unsatisfied bonding forces at a surface ". Surface tension: (γ): Surface tension is defined as the force (F) acting at right angle to a line of unit length (L) drawn in the surface i.e. $\gamma=F/L$. The surface tension is equivalent to surface energy under isothermal condition [8].

For relatively small droplets, the liquid droplet will assume an equilibrium confurigation dictated by surface free energy consideration. In the above case it is assumed that it is an idealized case i.e. where there are no chemical reaction between solid, liquid, and vapor phases, and the gravitational forces can be ignored. The shape of the liquid droplet is characterized by 'θ' the

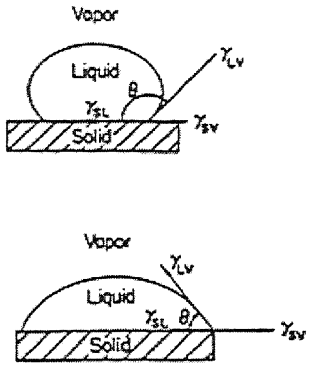

Figure [1] Surface tension forces acting when a liquid droplet wets a solid surface, according to the classical model. (8)

contact angle with the solid as shown in the Figure:1. The relationship between contact angle 'θ' and the surface free energies at the liquid-vapor (γ_{LV}), solid-vapor (γ_{SV}), and solid-liquid (γ_{SL}) interfaces is expressed by Cos $\theta = (\gamma_{SV}-\gamma_{SL})/\gamma_{LV}$ .The boundary between wetting and non-wetting conditions is generally taken as $\theta=90^0$. When $\theta<90^0$, wetting occurs, while when $\theta>90^0$ represents a condition of non-wetting. When θ approaches 0^0 spreading of liquid occurs. For most brazing systems the optimum value of θ is in the range of $10\text{-}45^0$.

Factors Affecting Contact Angle (θ): (a) Joint gap, (b) Surface impurity, (c) Presence of oxide & (d) Wettability Index (WI).

Joint gap: The thinner the joint gap, smaller will be 'θ' the contact angle and so we get a better wetting of the base material.

Surface impurities: Taking into consideration the equation,

$$Cos\theta = \frac{\gamma_{SV} - \gamma_{SL}}{\gamma_{LV}} eq \Rightarrow 1$$

It is clear that by increasing γ_{SV} i.e. the surface energy of solid-vapor interface we get a small value for 'θ', and γ_{SV} can be increased by having a clean surface and their maintenance by brazing in vacuum is apparent. The surface contamination impedes the wetting capability of the filler metal and must be removed for successful brazing. Cleaning can be done by mechanical means such as grinding, filing, wire brushing or any form of machining and by chemical means. Protective electroplating may follow chemical cleaning. Surface protection can also be done by the use of solid and liquid "Brazing fluxes".

Presence of oxide films: All real surfaces of liquid and solids are modified to some extent by absorption of surface-active elements and particularly oxidation. The presence of oxide on a solid metal surface suppresses wetting and inhibits spreading of liquid metal over the surface. Therefore much of the technology of brazing is directed to eliminate possible detrimental effects of oxide presence on wetting.

Wettability Index (WI): WI developed by Feduska [9] is used as the measure of the wettability . WI is defined as the area covered by the filler braze metal times the cosine of the contact angle between the braze and the base metals. So for high value of WI there is good wettability. WI depends on the volume of the filler metal used. WI greater than 0.05 are indicative of good performance during brazing, however when it is greater than 0.01 it is an indication of excellent performance during brazing [9]. In some cases, the wetting of a surface is much more complex and use of the above classical model i.e. the theory of wettability with respect to contact angle, is not so simple when chemical reaction between the filler metal and solid surface

takes place. The effect of metallurgical interaction between the filler metal and the component material in promoting wetting is exploited in active filler metals. The addition of small fraction of a reactive metal such as Ti or Zr to filler metal enables them to wet and spread over ceramic materials. In this instance wetting of and reaction with the ceramic are inextricably linked [11].

1.3 Capillary action:

Capillary attraction is the physical force that governs the action of a liquid against solid surfaces in small confined areas. Capillary flow is the dominant physical principle that ensures good brazements. When the joint gap at brazing temperature is proper, capillary force will be stronger than gravity and enable a liquid brazing filler metal, to be drawn between the faying surfaces of the joint in any direction, regardless of the orientation of the assembly (horizontal or vertical). The capillarity is a result of surface tension between the base metal(s), brazing filler metal, flux or atmosphere, and the contact angle between the base and filler-metals.

The vertical height to which a liquid rises between two parallel plates separated by a distance d is given by (10)

$$H = \frac{2\gamma_{LV}\cos\theta}{6\rho d} \Rightarrow eq-2$$

Where ρ= density of the liquid. The velocity v of the liquid into the space between two parallel surfaces of separation d is (10)

$$v = \frac{d^2 H}{8\eta h} \Rightarrow eq-3$$

Where h is the height, to which the liquid has risen,η is the kinematic viscosity given by (μ/ρ). The parameter μ is the viscosity of the liquid. It may be deduced that, other things being equal, the height to which a liquid rises in a capillary space increases as the separation of the surface is reduced and the rate of flow into the joint decreases as the separation of the surface is reduced.

In actual practice, brazing filler metal flow characteristics are also influenced by dynamic consideration involving fluidity, viscosity, vapor pressure, gravity and metallurgical reactions between brazing filler metal and base metal. (11). For capillary force to work, the base metal and the braze filler metal must be compatible, that is, they must be able to alloy with each other. The filler braze metal will then is able to "wet," or spread out along the surface of the base metal. The extent of alloying does not have to be much, but it must occur.

1.4 Joining atmosphere:

Controlled atmospheres are used during brazing to prevent the formation of oxides or other undesirable compounds. In most cases, controlled atmosphere are also used to reduce the oxides that permit the brazing filler metal to wet and flow on clean base metal. Controlled atmosphere brazing is widely used for the production of high-quality joints. In controlled atmosphere application post brazing cleaning is generally not necessary, and it avoids formation of oxides and scale over the whole part and often allow final machining to be done before brazing.

Recommended atmosphere composition is specified, wherever applicable and constitutes of mixture of various gases at particular required composition. The gases are H_2, N_2, CO, CO_2, and water-vapor (H_2O), CH_4, inert gases.

Vacuum is another form of controlled atmosphere and an increasing amount of brazing is being done in vacuum. Although many controlled atmospheres are available, those used primarily for brazing fall into three broad categories: (a) reducing atmosphere, (b) inert atmosphere and (c) vacuum. In some joining process oxidizing process is desirable, such as copper-copper oxide brazing process, where brazing is carried out to a ceramic material. A reducing atmosphere is one that is capable of chemically removing surface contaminants from the base materials. But there is some risk when dealing with hydrogen because of the hydrogen embrittlement and explosion at high temperatures.

Mizuhara et al [12] have suggested that Ti readily reacts with oxygen, nitrogen, and water vapor in the brazing process. Consumption of Ti by interaction with the above depletes the amount of Ti available to wet the ceramic surface, and the reaction product can also form on the surface of the brazing filler metal, which may prevent physical contact between Ti and ceramic part of the assembly. As a result, bonding with the ceramic will be poor. It has also been indicated that one of the best atmospheres for active brazing is a vacuum of level 10^{-5} torr and leak rate of the vacuum furnace should be less than 0.67 Pa per hour.

1.4(a) Vacuum Brazing: Vacuum brazing is economical for flux less brazing of many similar and dissimilar base metal combinations, especially for brazing very large, continuous area or complex assemblies where removal of solid or liquid flux is difficult and where there is inability of providing proper gaseous mixture. Vacuum is also suitable for brazing ceramics and reactive and refractory base metals such as Ti, Zr, Mo, Ta, etc. Vacuum brazing has the following advantage and disadvantages compared with high-purity brazing atmospheres.

Vacuum removes essentially all gases from the brazing area, thereby eliminating the necessity of purifying the supplied atmosphere. Commercial vacuum brazing generally is accomplished at pressure varying from 10^{-6} to 0.5 torr (10^{-4} to 67.5 Pa) and above, depending upon the materials brazed, the filler metal being used, the area of the brazing interfaces, and the degree to which gases are expelled by the base metals during brazing cycle.

Certain oxides of the base metal will dissociate in vacuum at brazing temperatures. Vacuum is widely used to braze stainless steel, superalloys, aluminium alloys, and with special techniques, refractory materials and ceramics.

Difficulties sometimes experienced with contamination of brazing interfaces due to base metal expulsion of gases are minimized in vacuum brazing. Occluded gases are removed from the interfaces immediately upon evolution from the metal.

The low pressure existing around the base and filler metals at elevated temperatures remove volatile impurities and gases from the metals, thus improving the property of the base metal. But this characteristic is a disadvantage where elements of the filler metal or base metals volatize at brazing temperatures because of the low surrounding pressures. This tendency may be corrected by employing partial pressure inert gas according to proper vacuum brazing techniques. Many vacuum furnaces have the ability to operate under a partial pressure of inert gas.

1.5 Prime Factors Controlling Brazing:

Temperature and Time: The temperature of the brazing filler metals of course must be above the melting point of the brazing filler metal and below the melting point of the parent metal. This temperature plays an important

role with regard to the wetting action and flow of the filler metal, the wetting and alloying action improves as the temperature increases.

Braze filler metals can be fairly complex alloys and their melting can take place over a range of temperature. Lower brazing temperatures are preferred to minimize heat effect on the base metal, increase the life of the fixture, jigs or other tools, minimize base metal/filler metal interaction etc. Higher brazing temperatures may be preferred to promote base-metal interaction in order to modify the brazing filler metal, permit subsequent processing at elevated temperatures, use a higher- melting but more economical brazing filler metal. There are two opposing factors in determining the maximum brazing temperature. The higher the temperature, the more active the ABA, and therefore, the better the wettability. Conversely, the higher the temperature, the more alloying occurs with the metal member, and the braze alloy has a lower viscosity. In very general terms, a temperature between 20-25^{0}C above the braze alloy liquidus nearly always gives good results.

The time at the brazing temperature also affects the wetting action, particularly with respect to the creep of the brazing filler metal. If the filler metal has a tendency to creep, the distance generally increases with time.

Joint Design and Clearance: Brazing a ceramic material to itself represents no special problems in joint design. However, a major concern when brazing ceramics to metals is the accommodation of residual stresses. A brazed joint is not a homogeneous body; it is a heterogeneous assembly composed of different materials with different physical and chemical properties. In the simplest case, it consists of the base metal and braze filler metal. After brazing, a boundary zone will be formed between the base materials. Due to diffusion processes, the composition, physical, and

chemical properties of the interface will be different from the base materials. This aspect should also be considered during joint design.

Clearance between the base materials is also an important factor, because without clearance, the braze filler metal flow will be restricted and results in voids or shrinkage cavities in the joint after solidification. Therefore a small clearance and thin filler metal films provides sound joint.

On the other hand, thermal expansion of dissimilar base materials is fundamentally important factor and complex. For example, in the ceramic to metal joining, there is a large difference of thermal expansion of ceramic and metal. During heating, the metal part will expand more than the ceramic part resulting in lesser clearance. During cooling, a stress field will develop in the interface region due to thermal mismatch and results in low joint strength. Mizuhara et al [12] have investigated the effect of Ti concentration in the Cu-Ag filler alloy on the peel strength. Peel strength was observed to be maximum at a Ti concentration of about 1.5wt-%. However, both below and above 1.5wt% Ti the peel strength was lower. According to them, plastic deformation of the brazing filler metal during cooling from the brazing temperature accommodates thermal expansion mismatch. Therefore, the increase in strength of the brazing filler metal that is due to excess Ti content leads to poor accommodation of thermal expansion mismatch and results in high residual stress and hence low joint strength.

1.6 Braze filler metals and general characteristics:

Brazing filler metal, as defined by the American Welding Society, is a metal to be added when making a braze. Brazing filler metals are metals or alloys that has liquidus temperature above $840^0F(450^0C)$ but below the solidus temperatures of the metals being joined. A Satisfactory brazing filler metal or alloy should posses the following characteristics:

(a) The ability to wet the base materials on which it is used.

(b) Suitable melting point or melting range and fluidity to permit its distribution by capillary attraction into properly prepared joints.

(c) A Composition of sufficient homogeneity and stability to minimize separation of constituents by liquation under the brazing conditions to be encountered.

(d) The ability to form brazed joints possessing suitable mechanical and physical properties for the intended service application.

(e) Depending on requirements, the ability to produce or avoid certain base metal/filler metals interactions. Brittle intermetallic compounds or excessive erosion may be undesirable, while higher joint remelt temperature might be an attribute.

The silver-based filler metals are primarily used to join most ferrous and non-ferrous metals, except aluminium and magnesium, with all methods of heating. They may be preplaced in the joint or fed into the joint area after heating. Lap joints are generally used with joint clearances of 0.5 to 0.13 mm when mineral type fluxes are used and upto 0.05 mm when gas phase fluxes (atmospheres) are used.

Copper wets and forms alloys with iron, cobalt, and nickel much more readily than silver does. Consequently the wettability of silver-copper brazing filler metals decreases as the silver content increases in brazing of steels, stainless steels, nickel-chromium alloys and other metals. Thus, high silver content filler metal doesn't wet steel well when brazing is done in air with a flux. When brazing is done in certain protective atmospheres without flux, Ag-Cu filler metals will wet and flow freely on most steels at the proper temperatures. Tin has a low vapor pressure at normal brazing temperatures. It is used in silver- based filler

metals in place of Zinc or Cadmium when volatile constituents are objectionable, such as when brazing is done without flux in atmosphere or vacuum furnaces or when the brazed assemblies will be used in high vacuum at elevated temperatures. Tin addition to silver-copper filler metals result in wide melting ranges. Filler metals containing zinc wets ferrous metals more effectively than those containing tin, and where zinc is tolerable, it is preferred over tin. [11].

Zinc and cadmium containing filler metals should not be used in a controlled atmosphere furnace. Filler metal Bag-1 containing 24 wt. % and 16 wt. % Zn showed some problem when used in brazing parts in a continuos furnace at 704-732^{0}C. The first problem with the filler metal containing cadmium is the use of higher concentration of approximately 24wt% considering that the metal Cd is poisonous. It readily dissociates from the filler metal and either deposits in the furnace as a powder or is carried out in the atmosphere; in both cases leading to a hazardous condition. Secondly, zinc that has a concentration of approximately 16-wt% (in filler metal Bag-1) also dissociates, thus leading up to 40% loss in the volume of the filler metal applied to the joint. Thirdly, an additional problem could be caused by continuous vaporization of the zinc and cadmium, adding to some porosity in the joint area.

1.7 Filler metal-parent metal interaction:

When stainless steels and the nickel- and cobalt-base alloys are brazed at temperatures of 1000-1200 ^{0} C, interaction between the molten filler metal and solid parent metal occur. This is especially the case when nickel- and cobalt-based filler metals are used.

A simple system, for example brazing of nickel is brazed with the eutectic alloy (89/11 Ni/P) at 1000 ^{0}C, can be used to explain the principles. From the constitutional diagram for Ni-P (Figure-2) it is seen that no equilibrium is possible between the molten filler metal of composition A and the parent metal (Ni) of composition E. The joint will consist of two solid nickel masses with eutectic Ni/P liquid in between. At each phase there

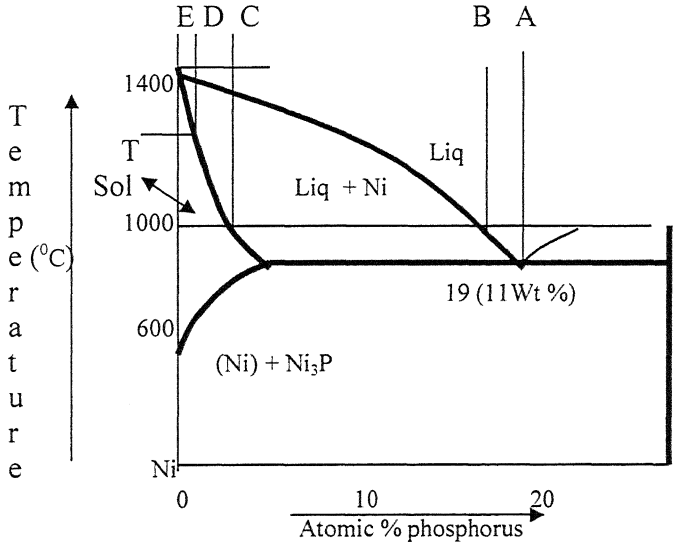

Figure [2]: Ni-P Constitutional Diagram (E.Lugscheido)[14]

will be a layer of composition C in between the eutectic and the nickel after a short time, for diffusion of nickel into the liquid and phosphorus into the solid. This will lower the phosphorus content of the liquid from A to B and raise the melting point to 1000^{0}C under the joint making conditions. After

heat treatment at 1000^0C and assuming there is much more nickel available than phosphorus, the surface of the parent metal will achieve composition D and will start to melt at T (the solidus), while the liquidus will be at C, and it will start to solidify at T.

Subsequent to the heat treatment, the interface will not start to melt until heated to T and the filler, which will start to melt at 875^0C, will not be completely liquid until T. Both of these changes will raise the failure temperature above what it was previously, perhaps 1000^0C with no load. The amount of eutectic will diminish during the heat treatment and if it is long enough, none will be left and no melting will occur below T. Similar, but more complicated, mechanisms takes place during brazing when B and Si temperature depressants are used.

1.8 Filler metal from binary alloy systems:

Binary eutectic compositions braze used with components of one of the constituent metals with no intermetallic compound formation. A representative example of this type of reaction is an Ag-Cu brazes used to join copper components. The Ag-Cu phase diagram is shown in Figure [3] [15]

Braze filler metals can be fairly complex alloys and their melting can take place over a range of temperatures. The implication of such behavior can be illustrated in terms of the phase diagram for Ag-Cu system as illustrated in the figure. Except for the eutectic composition (72%Ag-28%Cu), melting of the braze filler metals in this binary system occur over a range of temperatures as illustrated for the 50-50 composition.

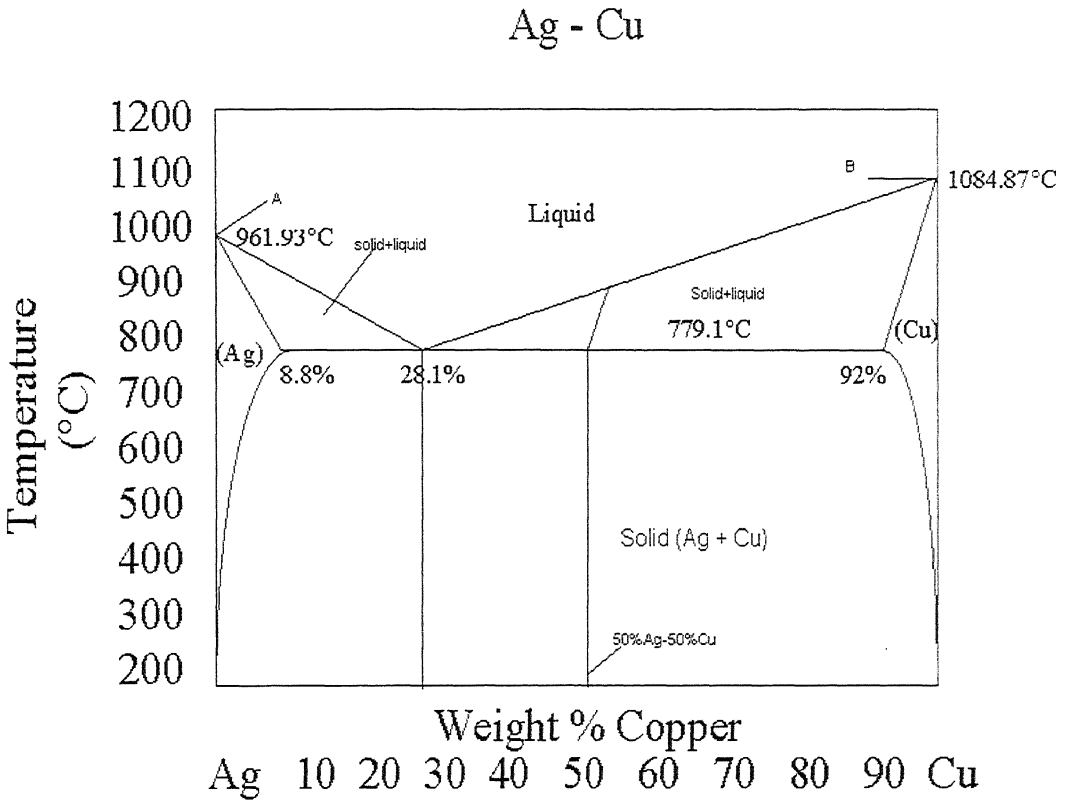

Figure 3. Silver-Copper phase diagram

Melting which begins at the solidus temperature of 780^{0}C is not complete until a temperature in excess of 850^{0}C is reached. Within the melting range there is a 'mushy' mixture of liquid and solid, which has wetting and flow properties distinct from those of the filler metal above the liquidus temperature. Flow in the partially melted filler is much reduced and the wetting and spreading tendency of the liquid phase in the mixture leads to the phenomena of liquidation or the tendency of the lower melting constituents. Liquidation results in melting point shifts and flow problems with the remaining higher melting constituents. The rate of heating through

the melting temperature range and the brazing time are important parameters, during brazing.

At the joining process temperature, the braze will dissolve copper until equilibrium concentration of Cu is reached. In this case, dissolution of Copper increases the liquidus temperature of the filler metal but not its solidus temperature because eutectic transformations are isothermal. On cooling below the liquidus temperature, the excess Cu-rich phase (β) will solidify first, and the precipitation will occur preferentially at the components/filler metal interface because heat lost via extremities of the assembly provides the interface to be slightly cooler. The precipitation will continue until the temperature and the composition of the remaining liquid reach the eutectic point.

Advantages of eutectic alloys as filler metals: The eutectic alloys have superior spreading behavior when molten and can be melted at a unique temperature and not over a range of temperature. The duplex character and the fine grain size of the eutectic microstructure, provides enhancement of both strength and ductility of a metal. The joining process temperature can be chosen to be only slightly above the melting point of the alloy. A rapid liquid to solid transformation on cooling, without going through the solid + liquid region. The alloying of the filler metal does not greatly shift the composition from its eutectic point.

2.Experimental procedure:

The aim of this investigation has been to join alumina to metals such as Nb, Ta, Cr, Co, Fe, Ni.etc.Cylinders of alumina 1.25cm in diameter and 1mm height were prepared by sintering green pellets for 3 hours at 1500^0C in a horizontal tubular furnace. The green pellets were prepared from alumina powder of >99% purity with the help of polyvinyl alcohol as binder at a pressure of 8 tons.

The filler metal used was a near eutectic alloy of composition, 60Ag-30Cu-10Sn from high purity metal. It was melted in silica capsules under vacuum. While melting the filler metal, the melt was continuously stirred to ensure a homogeneous alloy. The alloy ingot was then cut into 0.5mm thick discs.

While joining ceramic to metal, alumina was used as ceramic member and pure iron, niobium, nickel tantalum, zirconium etc were used as metal member. Discs of Titanium approximately 0.2mm thick was used as the active metal for better wetting of the alumina surface were obtained using a diamond cutter. Nickel and Niobium was used in rod form with 8mm diameter. Tantalum was in sheet form with thickness 1mm. The thickness of Co, Cr, Fe and Zr metals were around 1to 2 mm. The surface of the titanium disc was then polished on both sides using standard metallographic techniques to ensure optically flat surface for good bonding. The ceramic member (alumina), filler metal (Ag-Cu-Sn) and the metal member were also polished to ensure maximum area of contact between them for getting effective bonding. All surfaces of the sample were then cleaned in ultrasonic cleaner to make sure that no loose particles remain on the surface, which could hinder bonding.

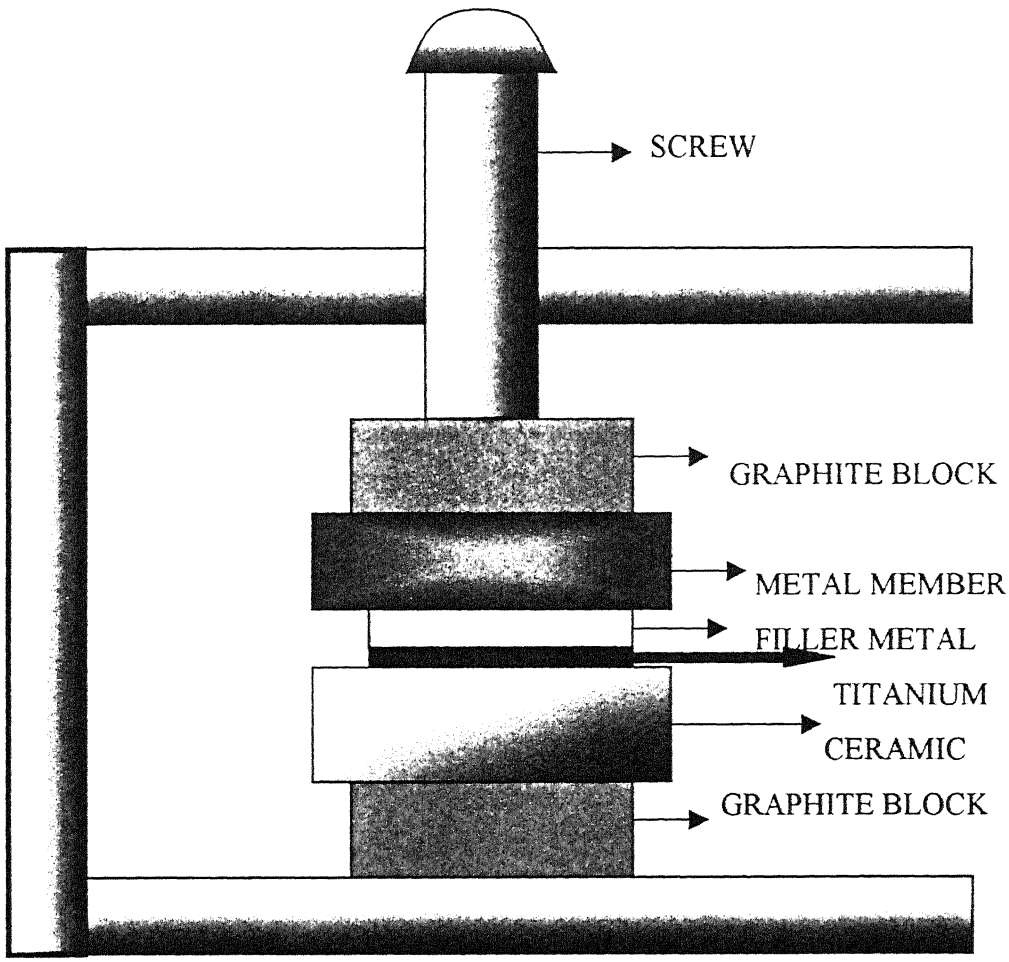

Figure [4]: Section of the assembly in which the specimen was prepared.

The samples were then kept in an assembly as shown in the Fig [4] .The sequence of the samples were as follows: the ceramic part was kept at the lowest position, above which the Ti slice was placed. It was followed by the filler metal and finally the metal part at the topmost position. Discs of graphite were kept one below the ceramic and the other at the top of the

metal to be joined with the ceramic and the assembly was tightened with a screw in a bracket shaped inconel plate.

The assembly was kept in a clean quartz tube and connected to a rotary vacuum pump. Vacuum of around 10^{-3} to 10^{-4} torr was obtained to control high temperature oxidation of the metals. The quartz tube was gently lowered inside a vertical furnace, which was already maintained at a fixed temperature of 900^{0}C.

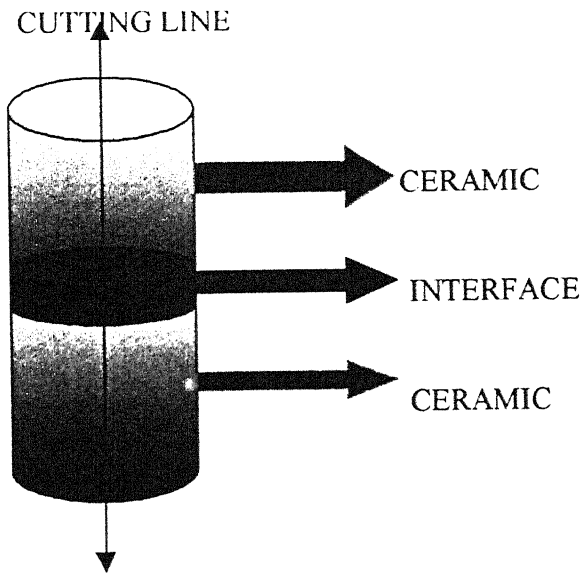

Figure [5]: The line along which the brazed specimen was cut to expose the interface

The multilayer diffusion couple was annealed for 16 hours at 800^0C. The quartz tube was taken out of the furnace and cooled in air till ambient temperature was reached. The cooling was done under vacuum. The diffusion couple was sectioned along the diamond cutter [Figure5]. It was subsequently polished using standard metallographic techniques.

The interface was studied using EPMA (electron probe micro analyzer). The compositions of the various phases were determined and the microstructures formed during solidification were recorded. The composition was studied using high purity standards of the metals.

3. Result and Discussion:

3.1 Al_2O_3/Ti/60Ag-30Cu-10Sn/Fe:

The ceramic Al_2O_3 was brazed with pure 'Fe' with braze filler metal 60Ag-30Cu-10Sn and Ti as the active metal at 800^0C for 16 hours. The interface was observed under EPMA and analyzed. The interface showed several phases in a complex microstructure of these phases and when analyzed gave several binary and some ternary intermetallic compounds. The formation of these compounds can be explained by diffusion. The composition of different phases was derived and the results are presented in table 2.

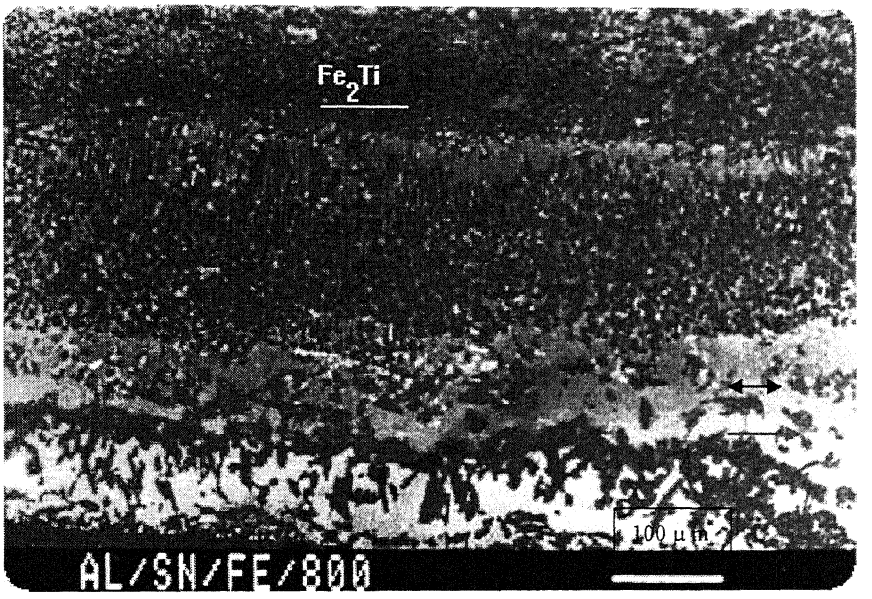

Figure [6a]: Photomicrograph of the Al_2O_3/Ti/60Ag-30Cu-10Sn/ (Fe) System, showing Fe_2Ti as dark particles in the upper part of the diffusion couple.

There are mainly 3 interfaces, Fe/filler-metal, filler metal /Ti and Ti/Al_2O_3. We scanned down, that is started analyzing the structure from the Fe phase down to the ceramic Al_2O_3 phase. The compound that was observed in the Fe/filler-metal interface was Fe_2Ti as dark particles seen in the photomicrograph, Fig. 6a, and Fig. 6b.

Serial no	Ag	Al	Cu	Fe	Sn	Ti	Identified phases	Structure and colour as viewed in EPMA
1	79.82	1.23	16.21	0.46	2.14	0.12	Ag rich solid solution +(Ag-Cu) eutectic	Bright region
2	20.14	0.51	75.20	0.54	1.48	2.13	(Cu)+(Ag-Cu) Eutectic	Gray matrix
3	00.19	0.003	0.29	68.31	0.13	31.06	Fe_2Ti	Dark particles
4	0.37	0.01	2.06	48.46	0.06	49.03	FeTi	Dark particles
5	0.10	0.00	10.31	40.30	0.20	49.08	Fe(Cu)Ti	Dark Particles
6	73.56	0.67	20.74	3.47	0.67	0.89	Ag+(Ag-Cu)	Bright region
7	0.66	0.004	42.74	16.25	0.09	40.25	Ternary phase	Thin dark particles
8	6.92	0.03	11.09	0.16	29.32	52.47	Ti_5Sn_3 in (Ag)	Gray particles in (Ag)
9	0.73	0.04	4.06	0.024	25.17	69.97	Ti_3Sn	Dark layer
10	2.37	0.00	30.99	0.00	0.08	66.55	Ti_2Cu	Dark gray layer
11	3.39	0.00	45.71	0.03	0.10	50.76	TiCu(Ag)	Less dark layer

Table 2: Composition (at%) of the elements in the different layers of the brazed specimen, alumina/Fe by using Ag-Cu-Sn as the filler metal taken by EPMA.

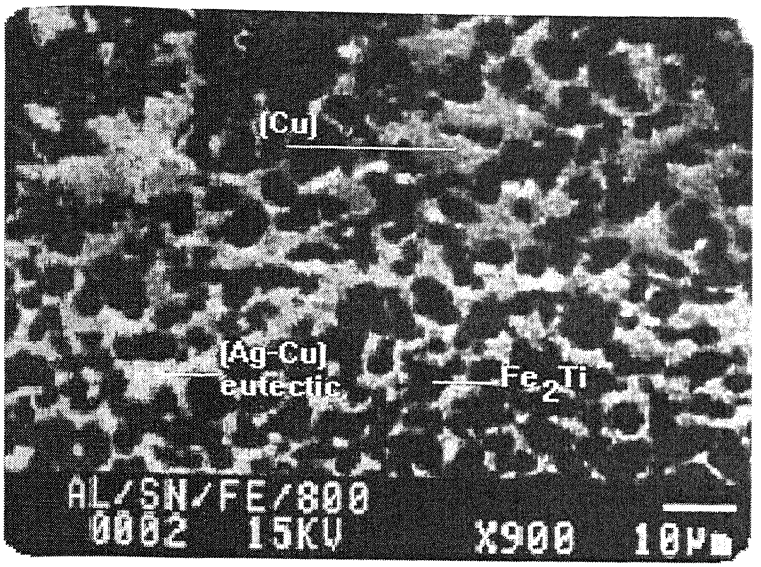

Figure [6b]: The photomicrograph of Al_2O_3/Ti/60Ag-30Cu-10Sn/Fe System, showing Fe_2Ti as dark particles, (Cu) and Ag-Cu eutectic.

The Fe_2Ti compound stoichiometry matches the compound $MgZn_2$ – type Laves phase and it melts congruently at 1427^0C; L $\longrightarrow$ Fe_2Ti. The composition of this phase obtained from the EPMA gave 68.31 at. pct. Fe in Fe_2Ti. The composition reported from the crystal structure data [16] shows a range of 64.5 to 72.4 at. pct. of Fe. The composition we obtained from the EPMA study matches with the composition given for the Fe_2Ti phase. It has also been reported [17] that alloys of composition near Fe_2Ti are very reactive.

The eutectic structure of the Ag-Cu system [18] is observed in the photomicrograph of Fig.7a. The eutectic reaction occurring at 779^0C, at 40 at. pct. Cu balance Ag has formed where as at other positions it shows a Ag-Cu eutectic structure in the matrix of Cu solid-solution, Fig.7b.

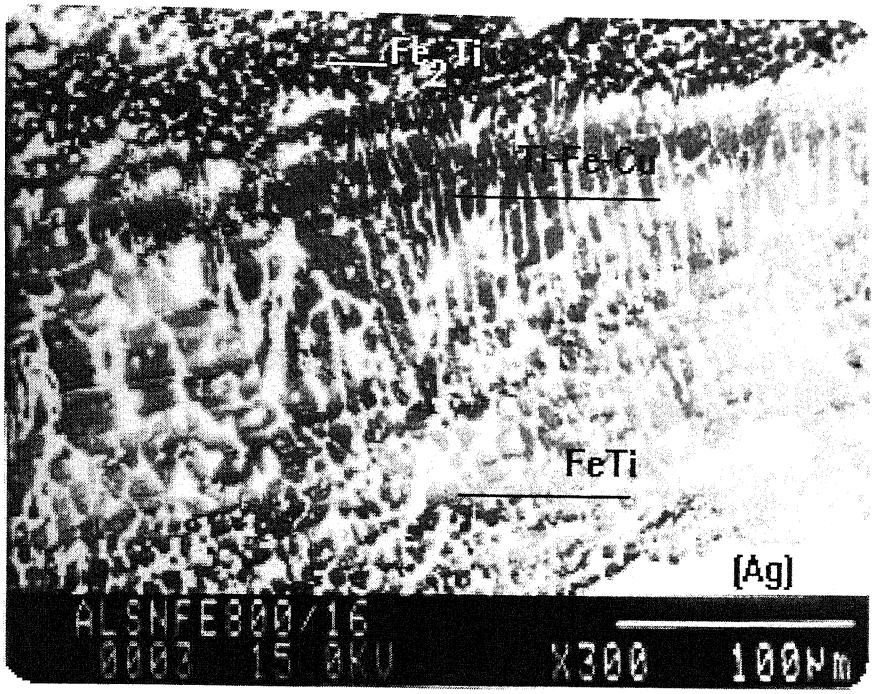

Figure [7a]: Photomicrograph of the Al_2O_3/Ti/60Ag-30Cu-10Sn/ (Fe) System, showing the upper part of the diffusion couple.

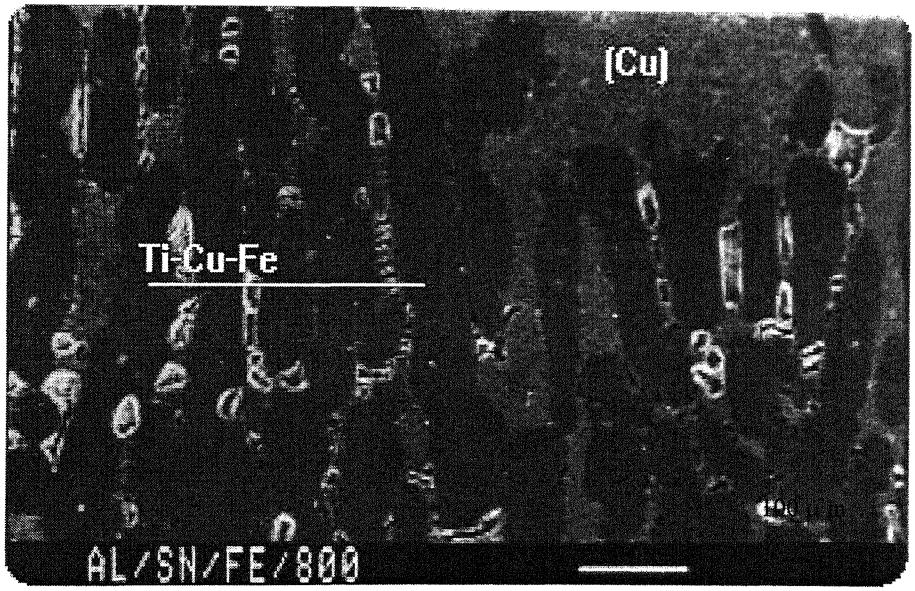

Figure [7b]: Photomicrograph of the Al_2O_3/Ti/60Ag-30Cu-10Sn/Fe System, showing the solid solution of Cu and dark particles of the unknown ternary of Ti-Cu-Fe.

The Ti-Fe phase diagram [16] shows that the compound FeTi and it forms from the melt by the peritectic reaction at 1317^0C.

$L+Fe_2Ti \longrightarrow FeTi$. The analysis of the FeTi phase has given 49.03 at. pct. Ti which is well within the range of the published composition [16]. At certain position, Cu was observed to substitute for Fe in the FeTi intermetallic. The Fe(Cu)Ti phase appears as a small dark particles in the photomicrograph, Fig.8a. The substitution of Cu was observed to be to the extent of 10.31 at. pct. Cu and when added to 40.30 at. pct. Fe it matches the range 49.8 to 52 at. pct. Fe reported for the FeTi phase [16].

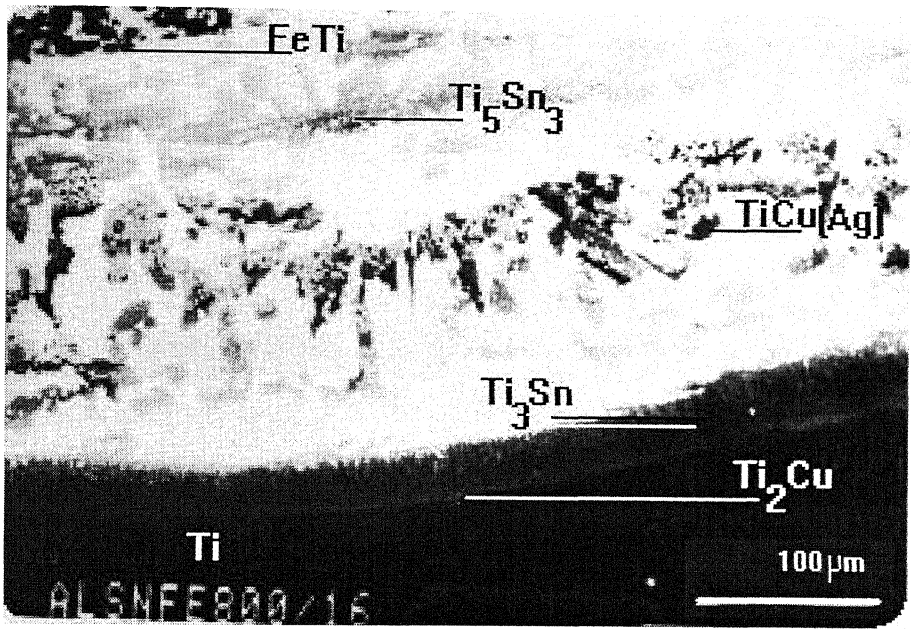

Figure [8a]: Photomicrograph of the Al_2O_3/Ti/60Ag-30Cu-10Sn/ Fe System, showing structure at and near the filler-metal/Ti interface.

As we scan down through the diffusion couple we see large bright regions of Ag solid solution Figs.8 a & b.

Between the bright silver solid solution, we have observed several phases. The gray particles have been analyzed to be consistent with the

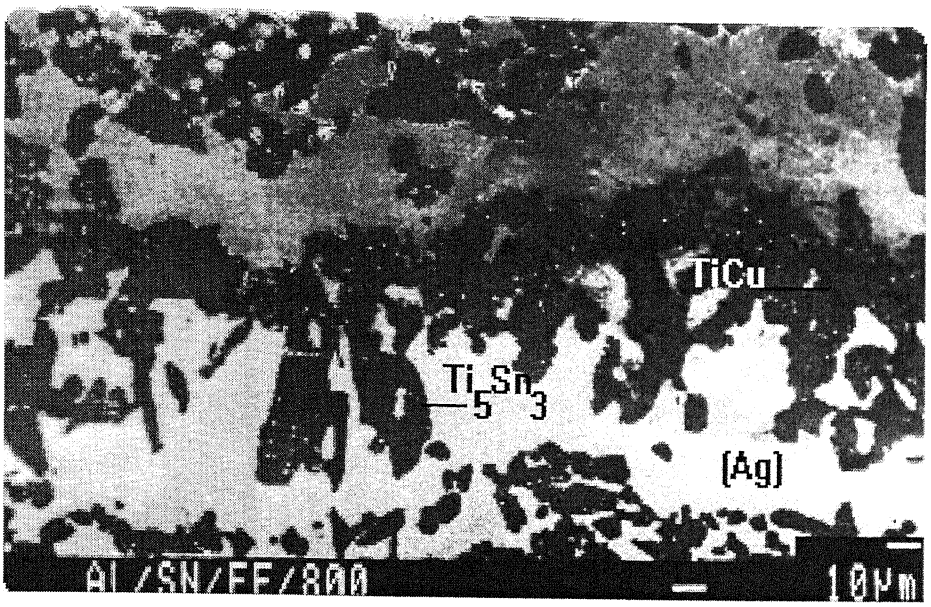

Figure- [8b]: Photomicrograph of the Al_2O_3/Ti/60Ag-30Cu-10Sn/ (Fe) System, showing dark particles of TiCu and gray particles of Ti_5Sn_3.

Ti_5Sn_3 phase, Figs 8a, 8b. The dark particles have been analyzed to correspond to the TiCu(Ag) phase, Fig. 8a and (table 2).The experimentally observed composition of the Ti_5Sn_3 phase gave a value of 29.32 at. pct. Sn and 52.47 at. pct. Ti which is close to the Ti_5Sn_3 composition reported in the literature [19]. The TiCu intermetallic and has been analyzed to show 50.76 at. pct. Ti and 45.71 at. pct. Cu. The reported composition [20] of this intermetallic with 48 to 52 at. pct. Ti and 48 to 52 at. pct. Cu agrees well with the observed composition. Upto 3.39 at. pct. Ag was observed to replace Cu in TiCu.

The Ti_3Sn phase has formed as a thick dark layer above the Ti/filer metal interface, Fig 8a. The composition observed for this phase is 25.17 at. pct Sn and 69.97 at. pct. Ti, table 2. The composition agrees with the reported composition for this phase [19]. The Sn concentration in the Ti_3Sn phase has a range from 23 to 25 at. pct. Sn.

The Ti_2Cu phase was obtained as thin gray layer just below the Ti_3Sn layer, Fig.8a. The observed composition 66.55 at. pct. Ti, 30.99 at. pct. Cu and 2.37

at. pct Ag with Ag substituting for Cu matches with the reported composition of Ti_2Cu phase [20].

A ternary phase was also observed in the photomicrograph, Figs. 7a, 7b, with a composition as shown in table 2.

3.2 Al_2O_3/Ti/60Ag-30Cu-10Sn/ Ni:

The ceramic Al_2O_3 was brazed with pure 'Ni' with braze filler metal 60Ag-30Cu-10Sn and Ti as the active metal at 800^0C for 16 hours. The diffusion couple was observed under EPMA and analyzed. The interface showed several phases in a complex microstructure of these phases and when analyzed gave several binary compounds. The formation of these compounds can be explained by diffusion. The composition of different phases was derived and the results are presented in table 3.

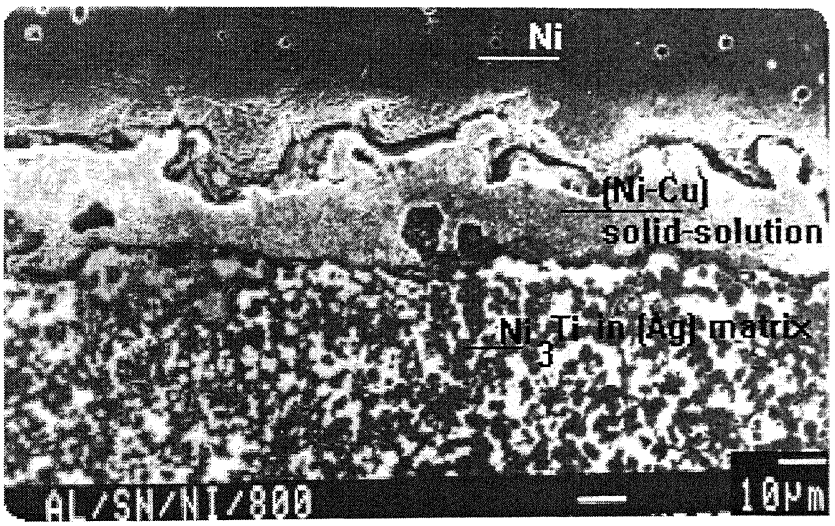

Figure-9: Photomicrograph of the Al_2O_3/Ti/60Ag-30Cu-10Sn/Ni System, showing dark particles of Ni_3Ti and gray layer of (Ni-Cu).

Serial no	Ag	Al	Cu	Ni	Sn	Ti	Identified phases	Structure and colour as viewed in EPMA
1	0.000	0.280	5.620	25.94	0.180	68.22	$Ti_2Ni(Cu)$	Light gray irregular structure
2	0.000	0.198	44.86	15.70	0.000	39.23	$Cu_3(Ni)Ti_2$	Large dark structure
3	0.000	0.025	1.64	69.67	0.02	28.65	$Ni_3(Cu)Ti$	Dark small particles
4	0.910	0.062	6.290	24.45	0.36	67.90	$Ti_2Ni(Cu)$	Light gray irregular structure
5	3.470	0.104	18.87	10.26	0.405	66.87	$Ti_2Cu(Ni)$	Dark matrix
6	0.600	0.123	1.254	0.545	23.95	73.53	Ti_3Sn	Light gray
7	2.000	0.199	38.35	7.170	1.250	51.02	TiCu(Ni)	Light gray globules
8	86.94	0.527	10.65	1.485	0.340	0.048	Ag Solid Sol. +10.6%Cu	Bright
9	2.920	0.122	17.91	75.72	0.000	3.318	Ni-Cu Solid Sol.	Gray layer

Table 3: Composition (at%) of the elements in the different layers of the brazed specimen, Alumina/Ni by using Ag-Cu-Sn as the filler metal taken by EPMA

We scanned down, that is started analyzing the structure from the Ni phase down to the ceramic Al_2O_3 phase. A Ni-Cu solid solution was observed near the Ni/Filler metal interface as a gray layer, Fig. 9.

The dark particles, in the middle of the filler metal region as shown in Figs. 9 and 10, are $Ni_3(Cu)Ti$. The analysis has shown 1.64 at. pct. Cu, 69.97 at. pct. Ni and 28.65 at. pct. Ti with small amounts of Ag, Al and Sn for this phase. The metal Cu substitutes for Ni in this phase. The Ni_3Ti

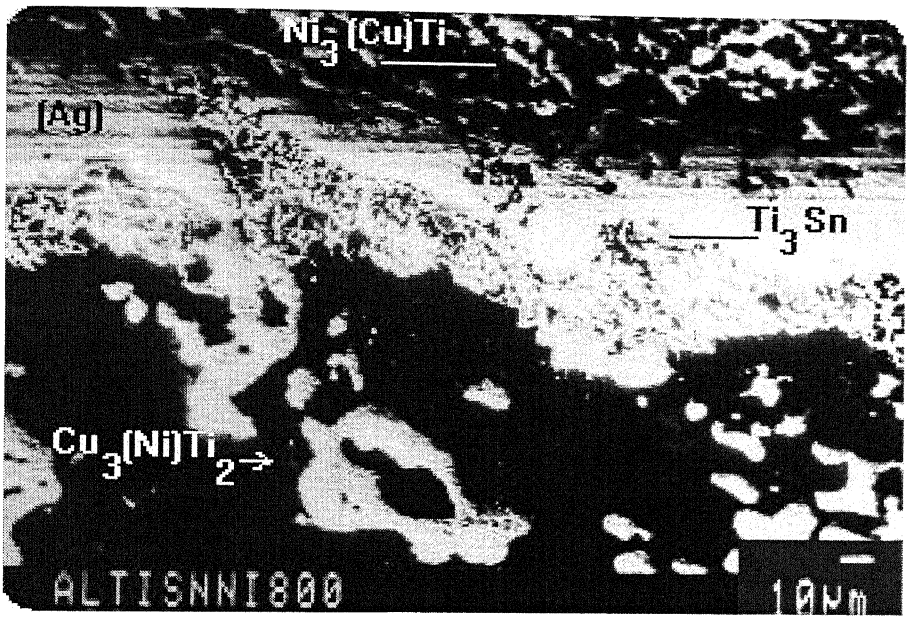

Figure [10]: Photomicrograph of the Al_2O_3/Ti/60Ag-30Cu-10Sn/Ni System, showing dark particles of $Ni_3(Cu)Ti$ and large dark region of $Cu_3(Ni)Ti_2$.

phase has been reported [22], with a composition of 75 at. pct. Ni balance Ti. The Ti concentration in this phase is observed to be higher than reported. [22] A stoichiometric compound $Cu_3(Ni)Ti_2$ is observed as large dark irregular region in the photomicrograph of Fig. 10. The observed composition shows 44.86 at. pct. Cu, 15.70 at. pct. Ni and 39.23 at. pct. Ti with small amounts of Ag, Al and Sn. Such large substitution of Cu by Ni is feasible because there is a complete mutual solubility of Cu and Ni in each other in the solid state. The published

composition of Cu_3Ti_2 intermetallic agrees well with that observed in this investigation if we assume Ni atoms substituting for Cu in the sublattice of the Cu_3Ti_2 intermetallic. From the phase diagram of the Cu-Ti system it can be seen that between the congruent melting of TiCu and the eutectic reaction at 73 at. pct. Cu, there is a cascade of peritectic reactions involving the compounds Ti_3Cu_4 , Ti_2Cu_3, $TiCu_2$ and $TiCu_4$ [20]. A light gray thin region of the Ti_3Sn phase with composition 23 at. pct. Sn and 73 at. pct. Ti has been observed in the diffusion couple, Fig.10.

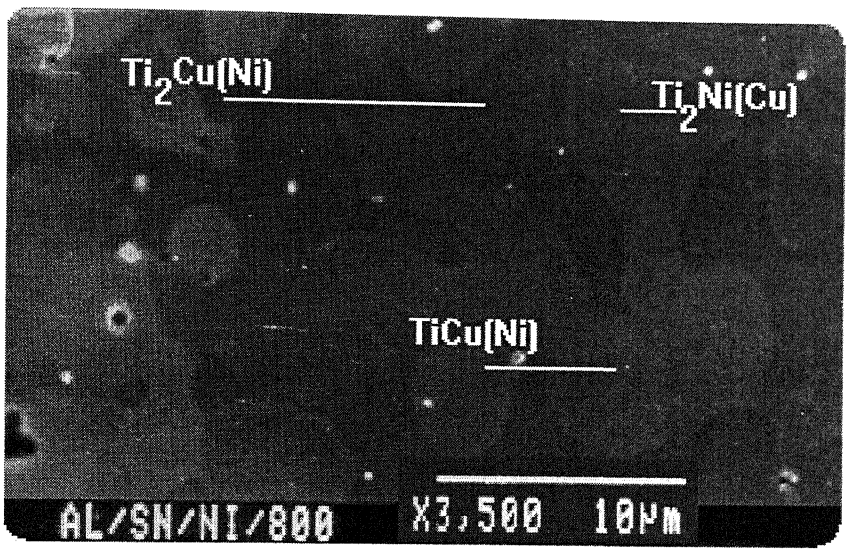

Figure [11]: Photomicrograph of the Al_2O_3/Ti/60Ag-30Cu-10Sn/Ni System, showing gray globules of TiCu(Ni) on dark Ti_2Cu(Ni).

The Ti_2Ni(Cu) compound forms as light gray irregular structure, Fig.11 near the Ti/filler-metal interface. The Ti_2Ni intermetallic has been reported to form by the following eutectic reaction at 942^0C. L $\longrightarrow$ (βTi) + Ti_2Ni. Experimentally we have obtained 24.94 to 25.94 at. pct. Ni, 5.62 to 6.29 at. pct. Cu and 67.9 to 68.22 at. pct. Ti with very small amounts of Al and Sn. Assuming that Cu substitutes for Ni in the Ti_2Ni phase the effective Ni concentration has a range of 30.74 to 31.56 at. pct. , which is close to the desired 33.33 at. pct. Ni for this intermetallic compound [22].

The Al_2O_3/Ti/60Ag-30Cu-10Sn/Ni diffusion couple also showed, light gray TiCu globules on the dark Ti_2Cu(Ni), Fig. 11. The morphology and reaction mechanism of TiCu phase has already been discussed while discussing the Al_2O_3/Ti/60Ag-30Cu-10Sn/Fe system. The Ti_2Cu phase shows a composition of 3.47 at. pct. Ag, 18.87 at. pct. Cu, 10.26 at. pct. Ni and 66.87 at. pct. Ti. Ni appears to substitute for Cu upto the extent of 14 at. pct. in this intermetallic compound.

3.3 Al_2O_3/Ti/60Ag-30Cu-10Sn/ Zr:

The ceramic Al_2O_3 was brazed with pure 'Zr' with braze filler metal 60Ag-30Cu-10Sn and Ti as the active metal at 800^0C for 16 hours. The interface was observed under EPMA and analyzed. The composition of different phases was derived and the results are presented in table 4.

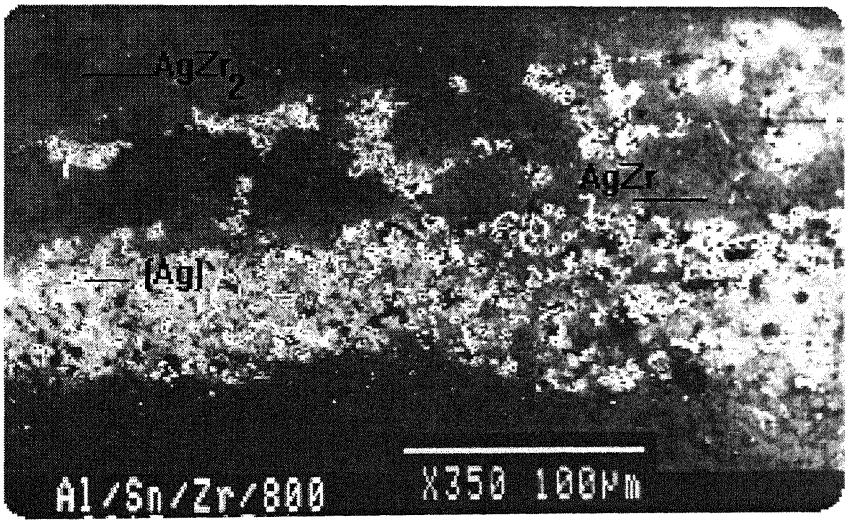

Figure [12]: Photomicrograph of the Al_2O_3/Ti/60Ag-30Cu-10Sn/Zr System, showing bright Ag solid solution and dark region of $AgZr_2$.

As we scan down from the Zr part of the diffusion couple we observe dark regions of $AgZr_2$, Fig. 12. The $AgZr_2$ compound has been reported to form by the following peritectic reaction at 1191^0C, L+ βZr $\longrightarrow$ $AgZr_2$ at 66 at. pct.

Serial No :	Ag	Al	Cu	Sn	Ti	Zr	Identified Phases	Structure and colour as viewed in EPMA
1	4.7	0.00	1.41	0.47	8.72	84.66	Zr	Gray
2	25.43	0.04	8.57	0.06	5.48	60.48	$Ag(Cu)Zr_2(Ti)$	Dark
3	30.71	0.00	7.25	0.067	5.90	56.06	$AgZr_2$	Dark regions
4	0.193	0.00	0.375	0.00	99.30	0.099	Ti	Dark region
5	1.18	0.02	9.8	33.57	2.72	52.68	Zr_5Sn_3	Gray oval particles
6	6.72	8.15	4.83	3.68	49.37	35.22	Ti-Zr solid sol.	Dark matrix
7	26.80	0.047	6.919	0.34	13.07	52.77	$AgZr_2$	Dark regions
8	4.38	0.10	3.97	3.28	63.01	24.50	Ti-Zr solid sol.	Dark matrix
9	45.00	0.600	3.600	1.540	17.40	31.72	Ag(Cu)Zr(Ti)	Light gray regions surrounding bright (Ag)

Table 4: Composition (at%) of the elements in the different layers of the brazed specimens, alumina/Zr by using Ag-Cu-Sn as the filler metal taken by EPMA.

Zr [23].Experimentally we have obtained 52.77 to 60.48 at. pct. Zr, 5.48 to 13.07 at. pct. Ti, 25.43 to 26.80 at. pct. Ag and 6.9 to 8.57 at. pct. Cu with very small amounts of Al and Sn. Assuming that Cu substitutes for Ag and Ti substitutes for Zr in the $AgZr_2$ phase the effective Zr concentration has a range of 65.84 to 65.96at.pct., which is close to the desired 66.66 at. pct. Zr, for the $AgZr_2$ intermetallic [23].

The light gray region in Fig.12 surrounding the dark $AgZr_2$ phase is of Ag(Cu)Zr(Ti). The AgZr resembles the CuTi phase and it forms by congruent melting at 1135^{0}C [23]. Experimentally we have obtained a composition of 31.72 at. pct. Zr, 17.40 at. pct. Ti, 45.00 at. pct. Ag and3.6 at. pct. Cu. Assuming that 3.6 at. pct. Cu substitutes for Ag and 17.40 at. pct. Ti substitutes for Zr in the AgZr phase, the effective Zr concentration is 49.12 at. pct. Zr which is close to the desired 50 at. pct. Zr for the AgZr intermetallic. The enclosed bright regions are the solid solution of silver.

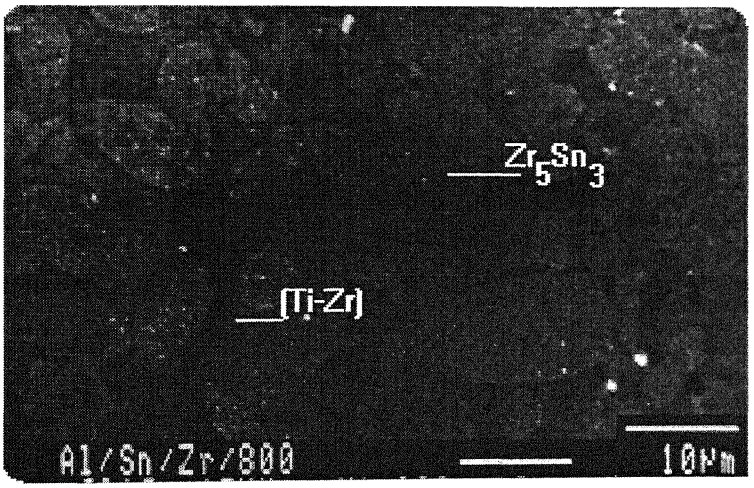

Figure [13]: Photomicrograph of the Al_2O_3/Ti/60Ag-30Cu-10Sn/Zr System, showing oval particles of Zr_5Sn_3 on dark Ti-Zr solid solution.

We have observed oval shaped dark gray Zr_5Sn_3 phase in a matrix of Ti-Zr solid solution near the Ti/filler-metal interface, Fig.13. The Zr_5Sn_3 is stable up to the congruent melting temperature of 1988^{0}C [24]. The composition reported

[24] for Zr_5Sn_3 phase shows a range of 33 to 40 at. pct. Sn. The observed composition in this study falls well within the reported range.

The dark gray matrix of Ti-Zr solid solution is observed in the photomicrograph of Fig.13. There is a range of composition of the Ti-Zr solid solution with Ti and Zr compositions falling in the range 49.37 to 63.01 at. pct. Ti and 24.5 to 35.22 at. pct. Zr. These composition lies in the β Ti-Zr solid solution range at 800^0C. The Ti and Zr metals are completely soluble in each other in all proportions as reported in the published phase diagram [25].

3.4 Al_2O_3/Ti/60Ag-30Cu-10Sn/ Nb:

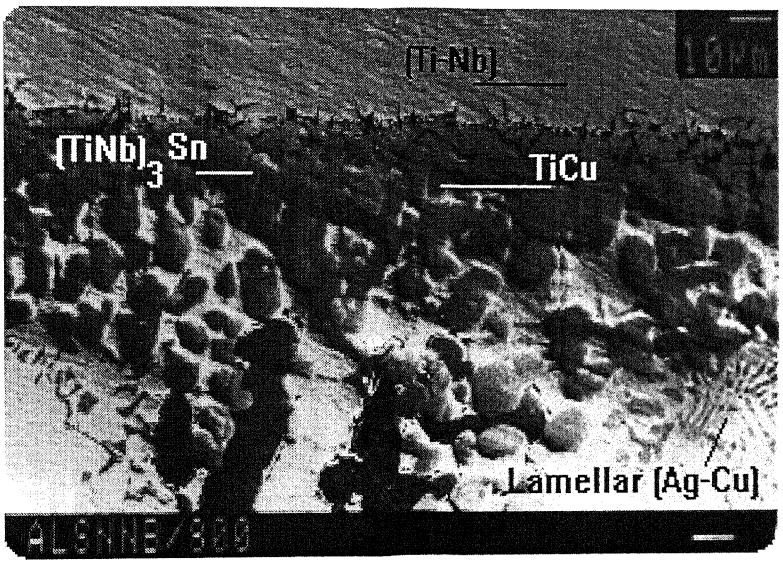

Figure [14a]: Photomicrograph of the Al_2O_3/Ti/60Ag-30Cu-10Sn/Nb System showing the upper part of the diffusion couple, showing the lamellar Ag-Cu and gray particles of $(TiNb)_3Sn$.

We analyzed the structure from the pure Nb down to the ceramic Al_2O_3. Just above the Nb/filler-metal interface, a dark layer of Ti-Nb solid solution has been observed as shown in the photomicrograph of Figs 14 a and b. The Ti-Nb phase diagram shows bcc (βTi,βNb) solid solution, with a complete range of solid

Serial No :	Ag	Al	Cu	Nb	Sn	Ti	Identified Phases	Structure and colour as viewed in EPMA
1	0.017	0.029	1.88	31.00	0.874	66.19	Ti-Nb solid solution	Gray in continuous with Nb
2	1.015	0.050	0.983	40.75	19.20	38.00	$(TiNb)_3Sn$+(Nb-Ti) solid solution	Gray particles just at the Nb/filler-metal interface
3	0.48	0.346	1.658	15.95	24.85	57.01	$(TiNb)_3Sn$	Gray particles
4	87.94	0.000	11.75	0.098	0.130	0.150	Ag solution	Bright
5	1.237	0.000	55.03	0.669	0.295	42.72	Ti_3Cu_4	Dark large region
6	0.167	0.018	11.18	3.585	32.62	52.52	Ti_5Sn_3	Light gray spherodial particles near Ti_3Cu_4
7	17.79	0.045	79.42	0.030	2.248	0.462	(Cu)+ (Ag-Cu)	Lamellar
8	0.718	0.018	4.435	0.208	24.00	70.61	Ti_3Sn	Gray continuous layer
9	0.144	0.065	46.53	2.947	0.305	50.06	TiCu	Dark surrounding the $(TiNb)_3Sn$
10	4.390	0.000	45.49	0.000	0.019	50.09	TiCu(Ag)	Gray particles just above the Ti_3Sn phase

Table 5: Composition (at%) of the elements in the different layers of the brazed specimens, alumina/Nb by using Ag-Cu-Sn as the filler metal taken by EPMA.

solubility above 882^{0}C. The stable equilibrium diagram is without an invariant reaction, congruent reaction transformation or critical points [26].

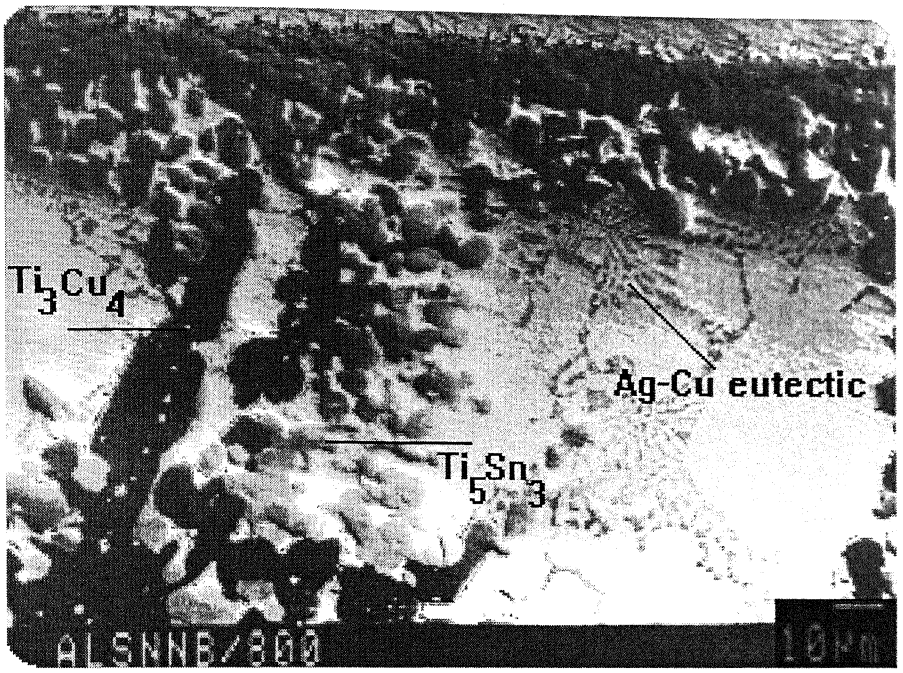

Figure [14b]: Photomicrograph of the Al_2O_3/Ti/60Ag-30Cu-10Sn/Nb System showing the large dark particle of Ti_3Cu_4 and gray particles of Ti_5Sn_3.

The dark nodular particles formed just below the Nb/filler-metal interface is the $(TiNb)_3Sn$ phase, Fig. 14 a. The analysis of the particles show a composition of 57.01 at. pct. Ti, 15.95 at. pct. Nb, 24.55 at. pct. Sn. It appears that about 16 at. pct. Nb has substituted for Ti in the sublattice of the Ti_3Sn intermetallic.

The dark region surrounding the $(TiNb)_3Sn$ phase is that of TiCu, Fig. 14 a. A Lamellar structure of the Ag-Cu eutectic, can be clearly observed in Figs. 14 a and b.

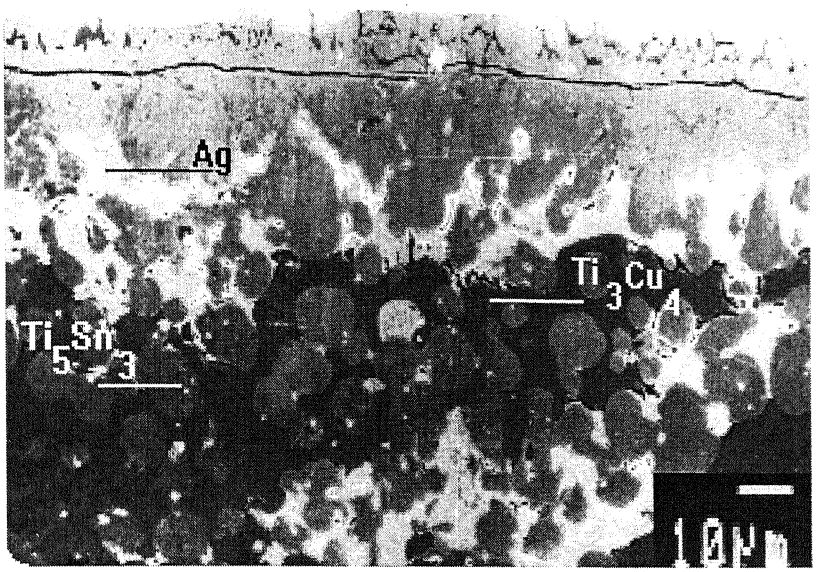

Figure [15]: Photomicrograph of the Al_2O_3/Ti/60Ag-30Cu-10Sn/Nb System showing the large dark particle of Ti_3Cu_4 and gray particles of Ti_5Sn_3.

The photomicrograph of Fig.15 shows spheroidal particles of Ti_5Sn_3 in a dark matrix of Ti_3Cu_4. The Ti_3Cu_4 is a stoichiometric compound, which forms by the following peritectic reaction, at 925^0C [20],

L+TiCu ⟶ Ti_3Cu_4 . Experimentally we have observed a composition of 42.72 at. pct. Ti, 55.03 at. pct. Cu and 1.237 at. pct. Ag. The composition obtained from the published data is 57.01 at. pct. Cu. [20]. The substitution of Cu was observed to be to the extent of 1.237 at. pct. Ag. When Ag is added to Cu it gives a composition close to the reported composition of 57.1 at. pct. Cu in the Ti_3Cu_4 phase [20].

The gray spheroidal particles of Fig. 15 on the Ti_3Cu_4 phase are the Ti_5Sn_3 intermetallic. The observed composition shows a mixture of the Ti_5Sn_3 and Ti_3Cu_4 intermetallic with 52.52 at. pct. Ti, 32.62 at. pct. Sn and 11.18 at. pct. Cu and small amounts of the elements Ag, Al and Nb.

While analyzing the Ti/filler-metal interface, we observed a gray continuous layer of Ti_3Sn

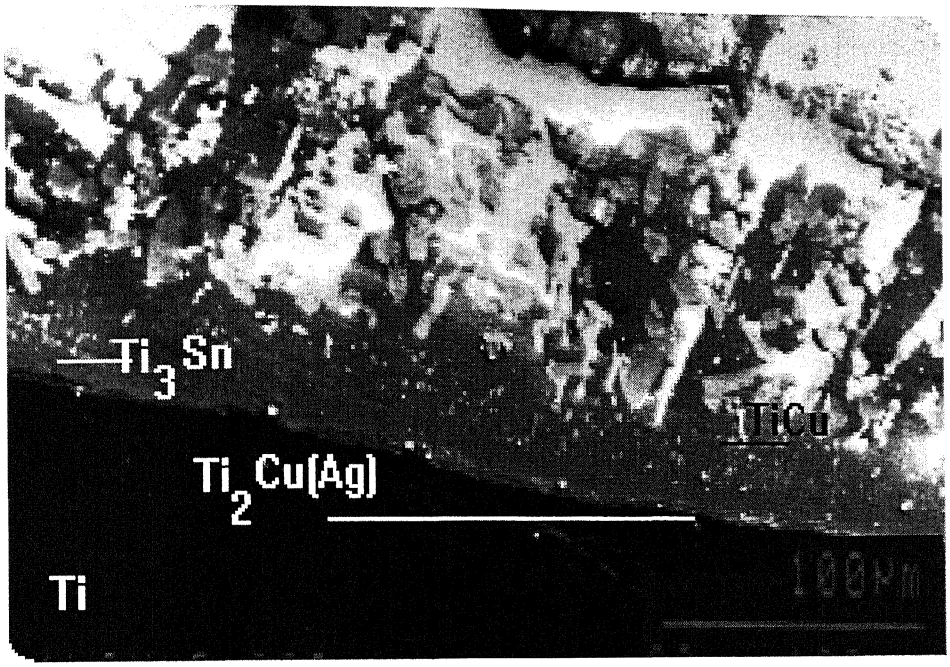

Figure [16]: Photomicrograph of the Al_2O_3/Ti/60Ag-30Cu-10Sn/Nb System showing the filler-metal/Ti interface.

followed by a light gray thin layer, which is assumed to be that of Ti_2Cu, Fig. 16. Experimentally we have obtained a composition of 24 at. pct. Sn and 70.61 at. pct. Ti for the Ti_3Sn. The Sn concentration as reported has a range from 23 to 25 at. pct. And it matches with the reported data, for this phase [19].

The TiCu(Ag) phase is seen as gray particles just above the Ti_3Sn layer, Fig 16.

3.5 Al_2O_3/Ti/60Ag-30Cu-10Sn/ Co:

We analyzed the diffusion couple starting from Co down to the ceramic Al_2O_3. The phase that was observed just below the Co/filler-metal interface was Ag-Cu solid solution shown as bright continuous layer as seen in the

Serial no	Ag	Al	Co	Cu	Sn	Ti	Identified phases	Structure and colour as viewed in EPMA
1	0.84	0.02	0.05	2.98	23.69	72.39	Ti_3Sn	Gray layer
2	4.04	0.00	0.00	44.50	0.27	51.0	TiCu(Ag)	Dark particles
3	0.00	0.102	71.79	2.10	0.023	25.97	$TiCo_3$	Dark irregular layer
4	0.00	0.73	99.06	0.98	0.04	0.67	Co	Gray
5	92.58	0.901	0.348	5.179	0.085	0.899	Ag Solution	Bright region
6	81.56	1.11	5.047	10.67	1.53	0.073	Solid-Solution : Ag-Cu	Bright continuous region
7	0.085	0.018	41.16	5.01	0.176	53.55	TiCo	Dark gray particles
8	0.049	0.024	46.89	3.215	0.267	49.55	TiCo(Cu)	Dark gray particles
9	0.817	0.051	0.458	4.375	0.765	93.53	Ti	Dark
10	3.400	0.060	0.270	9.120	28.13	58.98	Ti_5Sn_3	Light gray matrix with dark particles
11	0.120	0.200	31.18	17.14	0.243	51.27	TiCo+TiCu	Two phase structure

Table 6: Composition (at%) of the elements in the different layers of the brazed specimen, Alumina/Co by using Ag-Cu-Sn as the filler metal taken by EPMA

photomicrograph of Fig.17.The copper from the Ag-Cu eutectic composition must have reacted with the other elements Co, Ti etc.

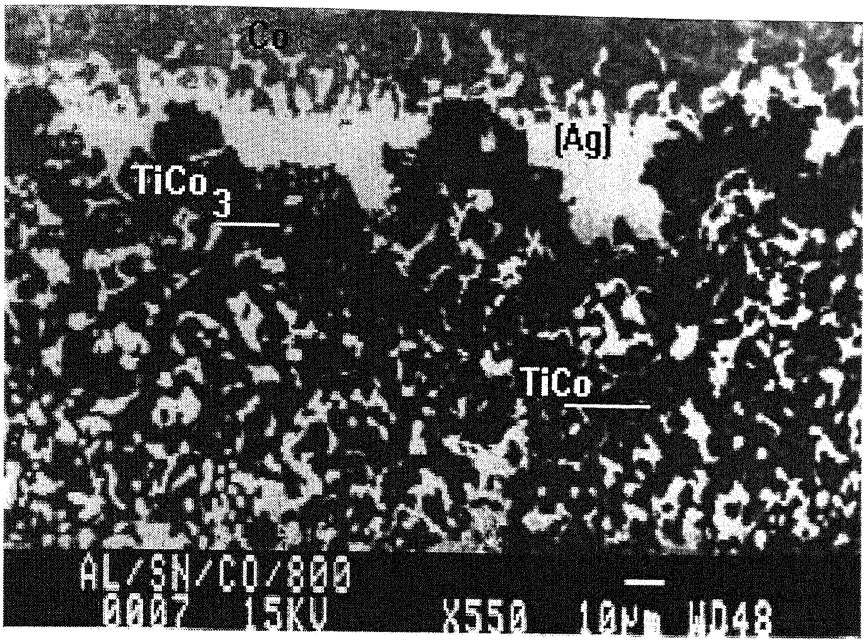

Figure [17]: Photomicrograph of the Al_2O_3/Ti/60Ag-30Cu-10Sn/Co System showing the large dark layer of $TiCo_3$ and dark particles of TiCo.

The $TiCo_3$ phase appears as irregular dark layer just below the Ag-Cu solid solution, Fig. 17. The $TiCo_3$ has an ordered fcc $AuCu_3$ -type structure and a maximum homogenity range of 75.5 to 80.7 at. pct. Co, [27]. The analysis has shown a composition of 71.79at.pctCo, 2.10 at. pct. Cu, 25.97 at. pct. Ti and small amounts of Sn and Al, for the $TiCo_3$ phase. It appears that approximately 2 at. pct. Cu substitutes for Co in the $TiCo_3$ intermetallic. According to the Co-Cu phase diagram, [28], Co can dissolve up to 3 at. pct. Cu at 800^0C, the temperature used for the diffusion anneal. The solubility of the third element in an intermetallic may change depending upon the element forming the other sublattice. However, we notice that the Co/Cu ratio of (97/3) in the Co-Cu solid solution is maintained in the $TiCo_3$ intermetallic, which is (71.79/2.1).

Just below the $TiCo_3$ phase, we have observed small dark particles of TiCo, Fig. 17, which has a CsCl structure, and melts congruently at 1325^0C [27]. The composition analysis shows a value of 53.55 at. pct. Ti, 41.16 at. pct. Co, 5.01at.pctCu and small amounts of Sn, Al and Ag in TiCo. The published data shows 48 to 56 at. pct. Co for this intermetallic at 800^0C. If we add Cu and Co concentrations, it gives a value of 46.16 at. pct. Co, which is close to the 48 at. pct. Co reported for this phase, [27]. But the solubility of Cu in Co is more in this case because of the open nature of the ordered bcc (CsCl) structure of the TiCo phase. From the composition data of the two observed Ti-Co intermetallic compounds it is apparent that Cu substitutes for Co in the sublattice of the TiCo and $TiCo_3$ intermetallics.

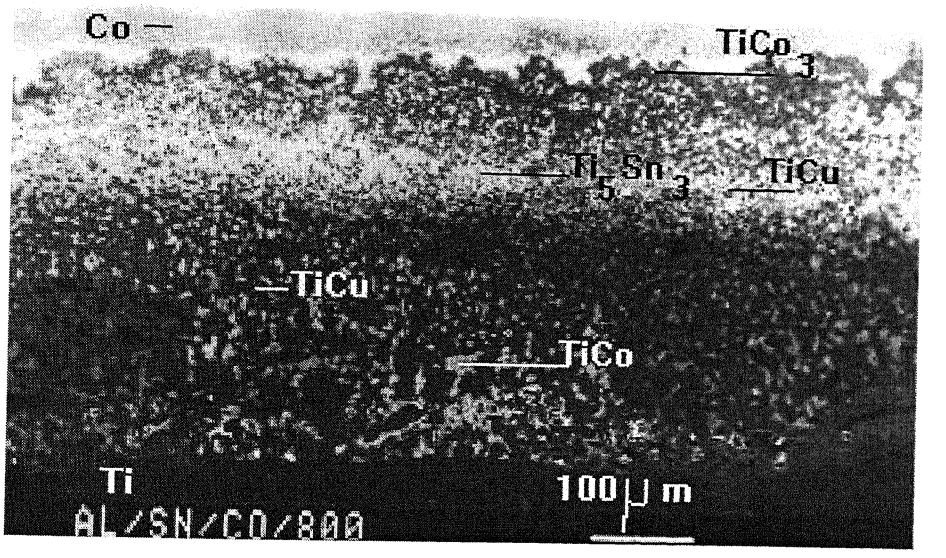

Figure [18]: Photomicrograph of the Al_2O_3/Ti/60Ag-30Cu-10Sn/Co System showing the whole diffusion couple.

The photomicrograph of Fig. 18 shows a gray continuous region and is analyzed to be that of Ti_5Sn_3. The dark particles on the gray are that of TiCu. The composition of the gray region with the dark particles is 58.98at.pctTi, 28.14 at. pct. Sn, 9.12 at. pct. Cu and 3.4 at. pct. Ag. The two-phase structure below the Ti_5Sn_3 layer corresponds to TiCo and TiCu with the light gray particles

representing the TiCo phase. The composition of this phase as shown in table 6, and it is 51.27 at. pct. Ti, 31.18 at. pct. Co and 17.14 at. pct. Cu and small amounts of Ag, Al and Sn.

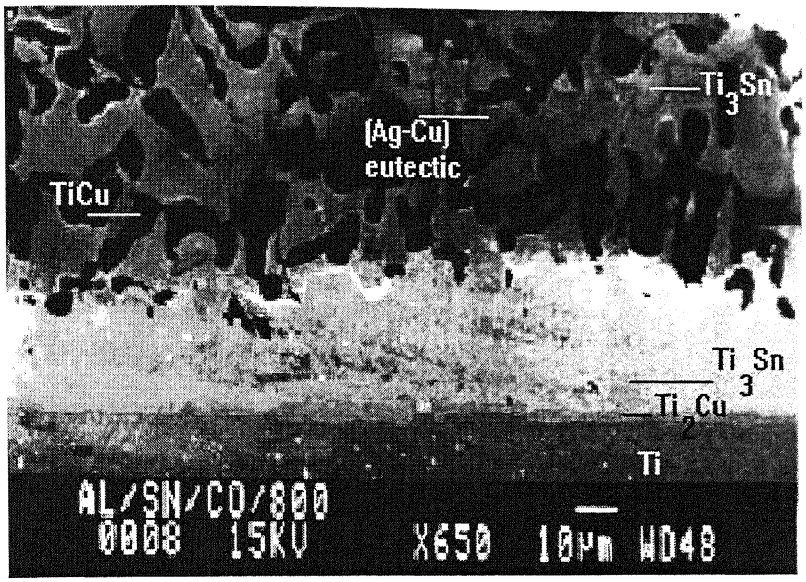

Figure [19]: Photomicrograph of the Al_2O_3/Ti/60Ag-30Cu-10Sn/Co System showing the lower part of the diffusion couple.

The photomicrograph of Fig.19 shows the light gray irregular particles of Ti_3Sn, dark particles of TiCu in the matrix of very fine rod like Ag-Cu eutectic. A very thin bright layer of Ag is also present, Fig.19. The Ag of the filler metal has diffused near the Co/filler-metal interface and (Ag) has formed with approximately 10.5 at. pct. Cu. The Cu content of the filler metal has combined with Ti to form the TiCu intermetallic. A gray layer of Ti_3Sn is observed below the bright (Ag) and a thin layer of Ti_2Cu, Fig. 19, follows it.

3.6 Al_2O_3/Ti/60Ag-30Cu-10Sn/ Cr:

The ceramic Al_2O_3 was brazed with pure 'Cr' with braze filler metal 60Ag-30Cu-10Sn and Ti as the active metal at 800^0C for 16 hours.

Serial no	Ag	Al	Cr	Cu	Sn	Ti	Identified phases	Structure and colour as viewed in EPMA
1	0.780	0.023	41.96	6.970	0.040	50.19	Ti-Cr Solid Solution	Dark particles
2	8.466	0.000	0.234	37.64	0.105	53.55	TiCu(Ag)	Dark particles
3	64.46	0.000	0.036	15.19	0.015	20.28	TiCu in Ag Solid Sol.	Dark particles
4	41.66	0.033	0.077	16.02	0.44	41.75	γCuTi + γAgTi	Dark continuous layer consisting of two phases
5	0.640	0.040	0.220	1.860	22.99	74.24	Ti_3Sn	Gray globules
6	88.76	0.000	0.140	3.390	1.430	6.260	Ag	Bright
7	5.175	0.016	0.054	25.68	0.259	68.87	$Ti_2Cu(Ag)$	*Dark globules*
8	0.000	0.000	11.790	33.90	0.000	54.00	Ti_5Cu_3Cr	Light gray in association with the Ag-Cu eutectic

Table 7: Composition (at%) of the elements in the different layers of the brazed specimen, Alumina/Cr by using Ag-Cu-Sn as the filler metal taken by EPMA

The structure of the interface was observed under EPMA and analyzed. The interface showed several phases in a complex microstructure. The composition of different phases was derived and the results are presented in table 7.

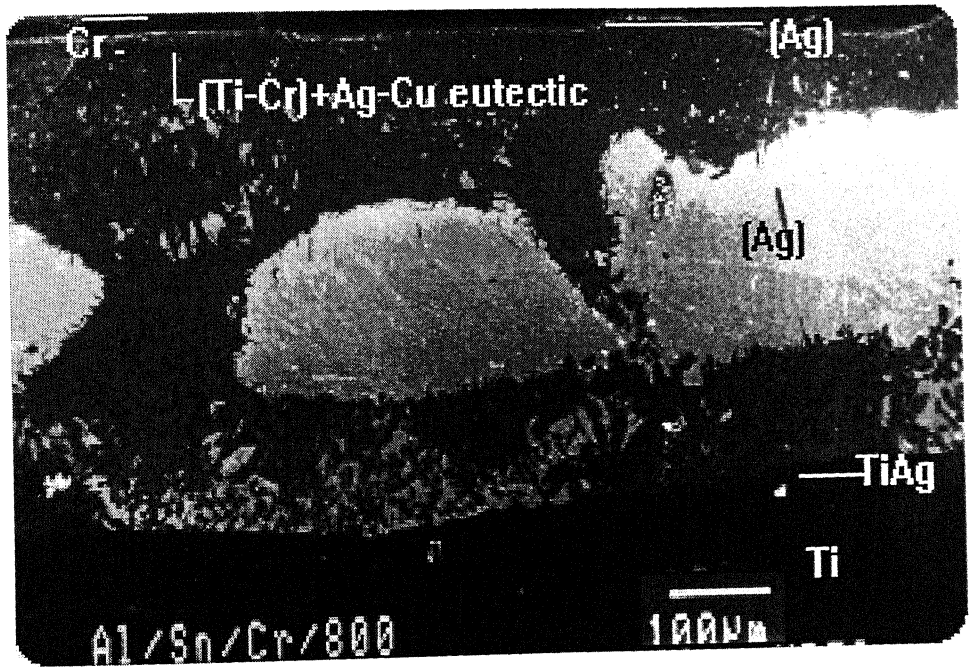

Figure [20]: Photomicrograph of the Al_2O_3/Ti/60Ag-30Cu-10Sn/Cr System showing the whole diffusion couple.

The microstructure was studied from pure chromium down to the Al_2O_3 ceramic. A very bright and thin layer of Ag solid solution has formed just below pure Cr, Fig. 20. Dark particles of the Ti-Cr phase with composition 50.19 at. pct. Ti, 41.96 at. pct. Cr, and 6.97 at. pct. Cu has formed just below the (Ag) layer. The Ti and Cr compositions lie close to the composition of the congruently melting alloy β(Ti,Cr) with 56 at. pct. Ti [29]. Approximately 7 at. pct. Cu appears to be substituting for Cr in the β(Ti,Cr) phase.

A three-phase region consisting of Ti_5Cu_3Cr, (Cu) and (Ag) has formed below the Ti-Cr solid solution. The Ag and Cu solid solutions appear as

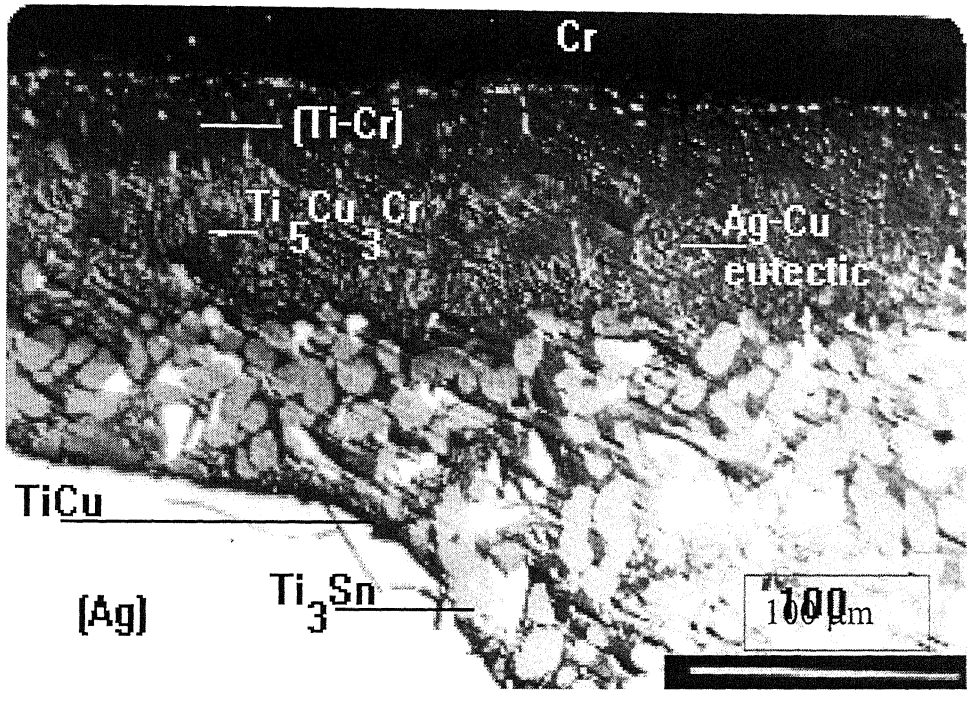

Figure [21]: Photomicrograph of the Al_2O_3/Ti/60Ag-30Cu-10Sn/Cr System showing the whole upper part of the diffusion couple with dark particles of TiCu and a ternary phase of Ti-Cr-Cu.

A three-phase layer consisting of the dark particles of TiCu, light gray globules of Ti_3Sn and Ag solid solution has formed in the middle of the filler metal region, Fig 21. The metal Cu has reacted to the extent that a broad bright region of Ag solid solution remains in the microstructure, Fig. 20 and 21. The composition of the Ti_3Sn phase and TiCu intermetallics are shown in the table-7.

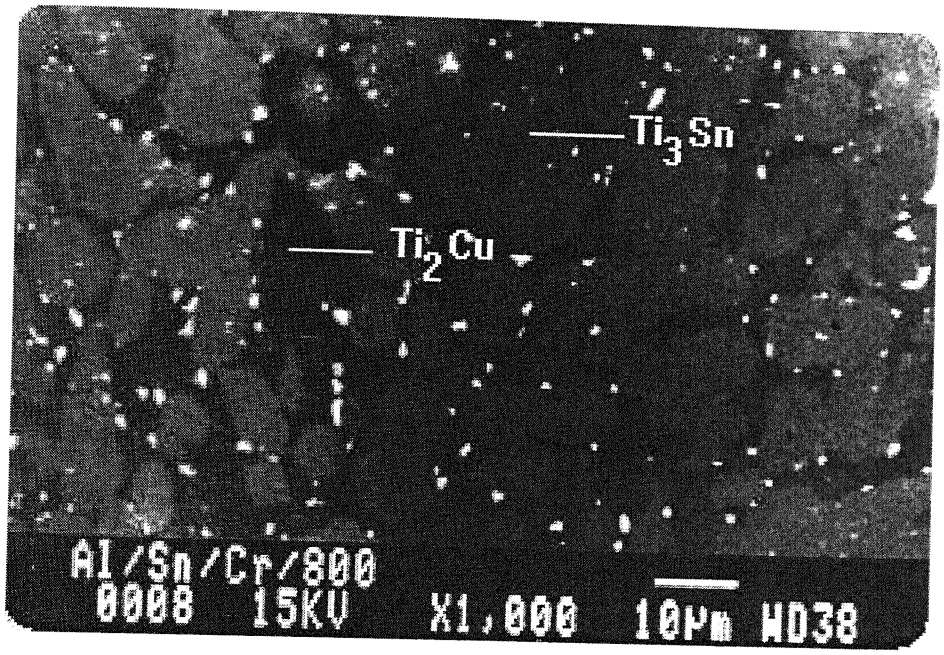

Figure [22]: Photomicrograph of the Al_2O_3/Ti/60Ag-30Cu-10Sn/Cr System showing dark particles of Ti_2Cu and gray particles of Ti_3Sn.

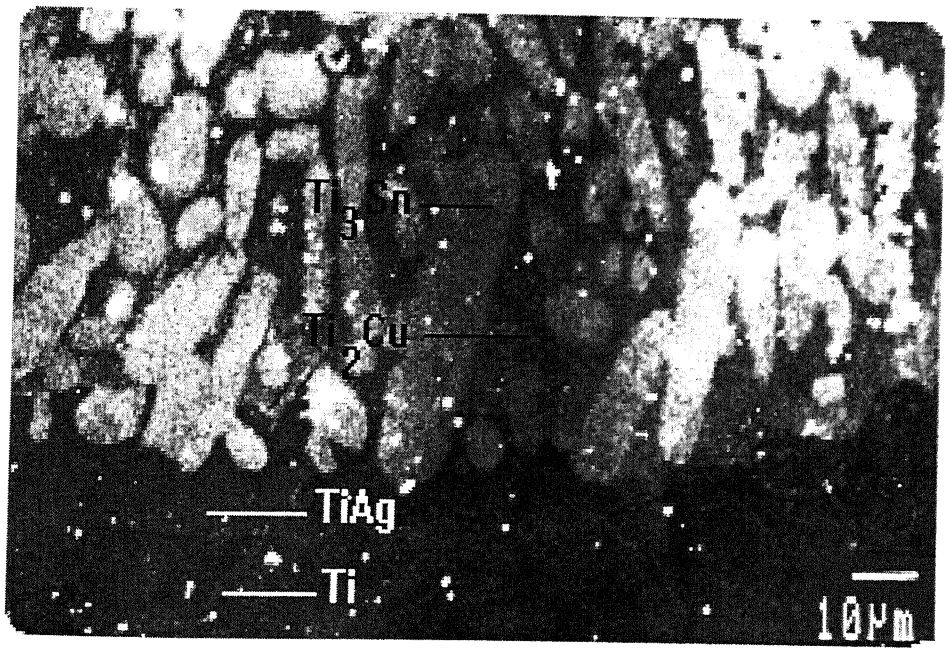

Figure [23]: Photomicrograph of the Al_2O_3/Ti/60Ag-30Cu-10Sn/Cr System showing the lower part of the diffusion couple dark particles of Ti_2Cu and gray particles of Ti_3Sn.

A two-phase layer consisting of Ti_2Cu and Ti_3Sn has formed as a next layer, Fig22. The Ti_2Cu appears as dark regions between the gray globules of Ti_3Sn. The composition of the Ti_2Cu shows that about 5 at. pct. Ag has substituted for copper in the Ti_2Cu phase, table 7.

A dark continuous layer of TiAg has formed just above the Ti layer, Fig. 23. It has been reported that the intermetallic TiAg has a γCuTi structure and a composition range of 48 to 50 at. pct. Ag [30].

3.7 Al_2O_3/Ti/60Ag-30Cu-10Sn/ Ta:

The ceramic Al_2O_3 was brazed with pure 'Ta' with braze filler metal 60Ag-30Cu-10Sn and Ti as the active metal at 800^0C for 16 hours. The interface was observed under EPMA and analyzed. The composition of different phases was derived and the results are presented in table 8.

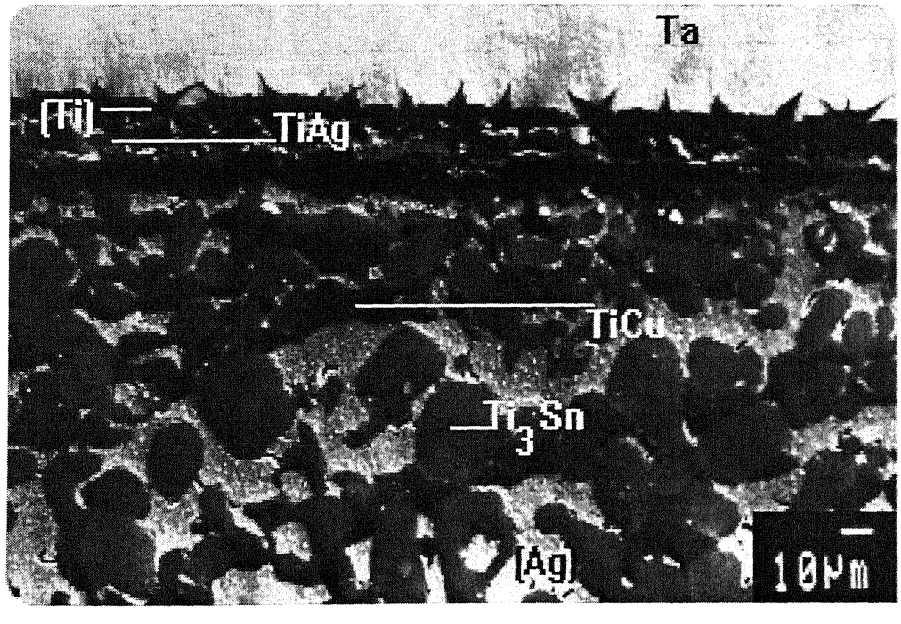

Figure [24a]: Photomicrograph of the Al_2O_3/Ti/60Ag-30Cu-10Sn/Ta System showing the Ta /filler-metal interface and dark layer of (Ti) at the interface and below the interface dark particles of TiCu and gray particles of Ti_3Sn.

Serial no	Ag	Al	Cu	Sn	Ta	Ti	Identified phases	Structure and colour as viewed in EPMA
1	0.948	0.062	0.177	23.480	0.910	74.42	Ti_3Sn	Gray particles
2	0.00	0.010	0.604	0.045	99.30	0.028	Ta	Bright gray
3	5.672	0.680	0.220	0.930	4.530	88.79	Ti solid solution	Dark layer with protrusion in Ta
4	2.606	0.078	46.27	0.3110	1.304	49.43	TiCu	Dark particles
5	90.67	0.070	8.797	0.1444	0.051	0.261	Ag solid solution	Bright matrix
6	3.176	0.210	31.06	0.134	0.000	65.41	Ti_2Cu	Dark continuous layer
7	0.000	1.715	0.145	0.300	0.168	97.66	Ti	Dark
8	32.91	0.149	4.034	15.711	0.904	46.28	Ti_3Sn in Ag solid solution	Light gray in bright matrix
9	13.67	0.100	3.030	20.86	1.580	60.73	Ti_3Sn in Ag solid solution	Light gray in bright matrix

Table 8: Composition (at%) of the elements in the different layers of the brazed specimen, Alumina/Ta by using Ag-Cu-Sn as the filler metal taken by EPMA

The photomicrograph of Figs. 24 a & b show the metal Ta, the Ta/filler-metal interface and the upper part of the filler metal. The bright large gray region was analyzed as Ta with composition of 99.30 at. pct. Ta, Fig. 24a. The light gray particles are Ti_3Sn in the matrix of Ag solid solution, Fig.24 a. Some of the Ti_3Sn particles appear faceted. The dark particles between Ti_3Sn are the TiCu intermetallic. The compositions of these two intermetallics are shown in table 8. The observed composition of 74.42 at. pct. Ti and 23.48 at. pct. Sn agrees well with the reported composition of the Ti_3Sn phase [19]. The TiCu phase has been analyzed to show 49.43 at. pct. Ti, 46.27 at. pct. Cu and 2.606 at. pct. Ag. The reported composition of this intermetallic with 48 to 52 at. pct. Ti agrees well with the observed composition [20]. The metal Ag upto 2.606at.pct. was observed to replace copper in the TiCu phase.

The light gray particles of Ti_3Sn in Ag solid solution with 46.28 at. pct. Ti, 15.71 at. pct. Sn, 32.9 at. pct. Ag and 4.034 at. pct. Cu has been observed near the Ta/filler-metal interface.

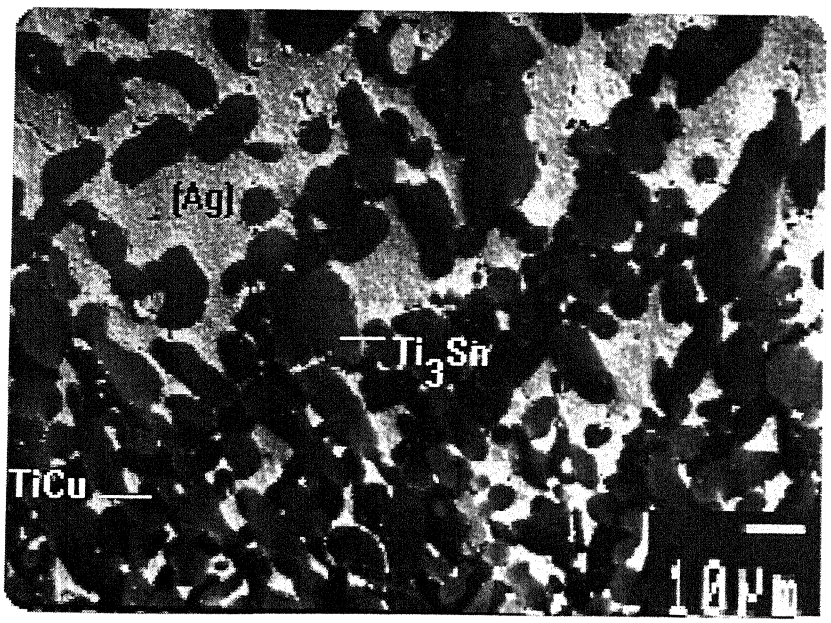

Figure [24b]: Photomicrograph of the Al_2O_3/Ti/60Ag-30Cu-10Sn/Ta System showing dark particles of TiCu and gray particles of Ti_3Sn in (Ag).

The dark layer just below Ta as seen in the photomicrograph of Fig 24 a, has been analyzed as Ti solid solution with composition 88.79 at. pct. Ti, 5.67 at. pct. Ag and 4.52 at. pct. Ta. It appeared that Ti has extensively diffused through the liquid filler metal to form a solid solution with Ta. The diffusion of Ta has been very limited. There is a complete solid solubility of Ta and Ti into each other in the whole composition [31]. The dark layer next to the Ti solid solution could not be analyzed but it is presumed to be the TiAg phase. This intermetallic has been observed near the base metal/ filler- metal interface in other diffusion couples.

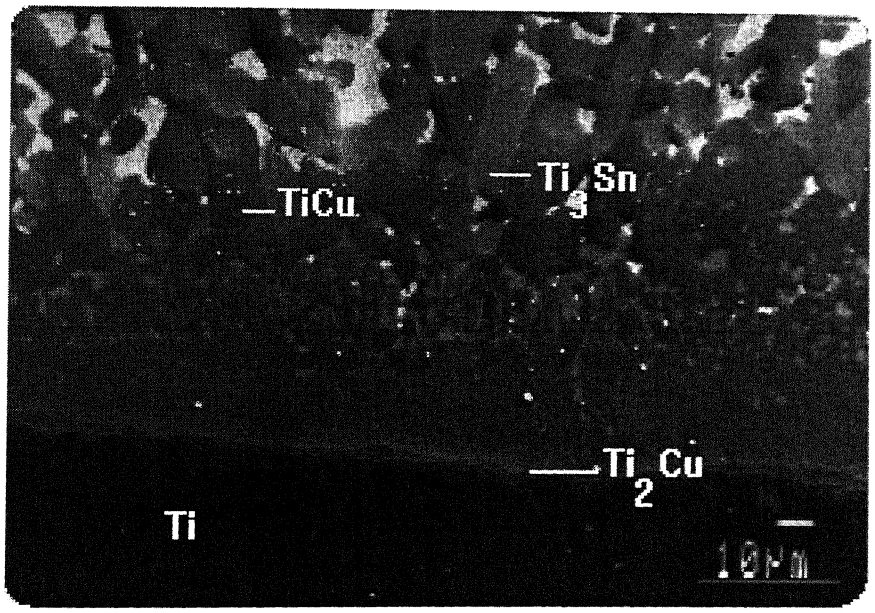

Figure [25]: Photomicrograph of the Al_2O_3/Ti/60Ag-30Cu-10Sn/Ta System showing the Ti/filler-metal interface and Ti_2Cu at the interface.

The photomicrograph of Fig. 25 shows formation of Ti_2Cu intermetallic just above the Ti/filler-metal interface as a dark layer. The Ti_2Cu phase shows a composition of 65.41 at. pct. Ti, 31.06 at. pct. Cu and 3.176 at. pct. Ag with Ag substituting for Cu. The composition agrees well with that reported for the Ti_2Cu phase [20].

The metal Ta has a melting point of 3020^0C, which is very high when compared to 800^0C, the temperature at which the experiment has been carried out. The diffusion of Ta was expected to be slow compared to the diffusion of the other elements Ti, Cu, Ag, and Sn. No intermetallic compounds of Ta are therefore observed.

3.8 Al_2O_3/Ti/60Ag-30Cu-10Sn/ Mn:

The ceramic Al_2O_3 was brazed with pure 'Mn' with braze filler metal 60Ag-30Cu-10Sn and Ti as the active metal at 800^0C for 16 hours. The interface was observed under EPMA and analyzed. The composition of different phases was derived and the results are presented in table 9.

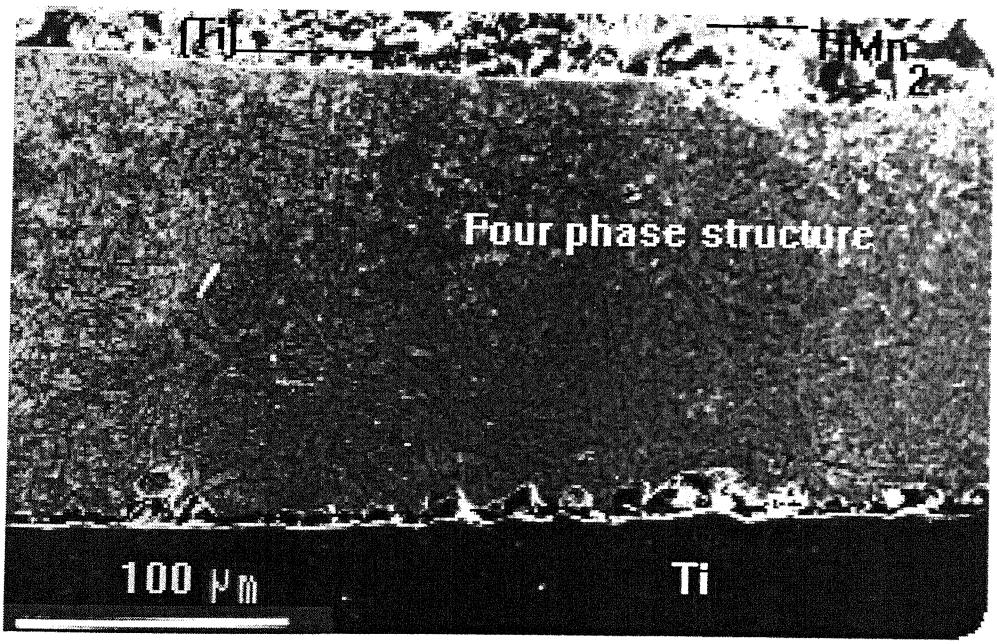

Figure [26]: Photomicrograph of the Al_2O_3/Ti/60Ag-30Cu-10Sn/Mn System showing the whole diffusion couple.

The photomicrograph of Fig. 26 shows gray particles of $TiMn_2$ above the uniform layer of the four-phase structure, described below. The $TiMn_2$ phase is

Serial no	Ag	Al	Cu	Mn	Sn	Ti	Identified phases	Structure and colour as viewed in EPMA
1	0.090	0.000	0.278	67.60	0.30	31.71	$TiMn_2$	Gray particles
2	0.000	0.040	0.856	18.27	0.300	80.50	(βTi)	Dark particles
3	0.019	0.166	0.933	4.668	0.088	94.13	(Ti)	Dark layer
4	55.80	0.099	17.80	23.19	3.046	0.054	Ag-Cu eutectic and Ag-Mn Solid Solution	A three phase structure
5	0.000	0.000	0.398	99.60	0.000	0.000	(Mn)	Dark
6	36.61	0.004	29.35	29.23	4.803	0.000	Ag-Cu eutectic, Ag-Mn Solid Solution	A three phase structure

Table 9: Composition (at%) of the elements in the different layers of the brazed specimen, Alumina/Mn by using Ag-Cu-Sn as the filler metal taken by EPMA

a Laves phase of the $MgZn_2$ – type with a homogeneity range of 60 to 70 at. pct. Mn and melts congruently at 1325^0C [32]. The composition obtained for this phase is 67.60 at. pct. Mn, 31.71 at. pct. Ti and small amounts of Ag, Cu and Sn.

The dark region surrounding the $TiMn_2$ phase is that of (Ti). It appears that Ti has extensively diffused through the liquid filler metal to form a solid solution, having composition of 80.50 at. pct. Ti, 18.2776 at. pct. Mn, and small amounts of the other elements. The Ti-Mn phase diagram shows that (βTi) solid solution has a solubility of 0 to 30 at. pct. Mn [32]. Y.Saleh and H.Margolin observed that a 9 at. pct. Mn alloy was a single-phase (βTi) at 700^0C [33].

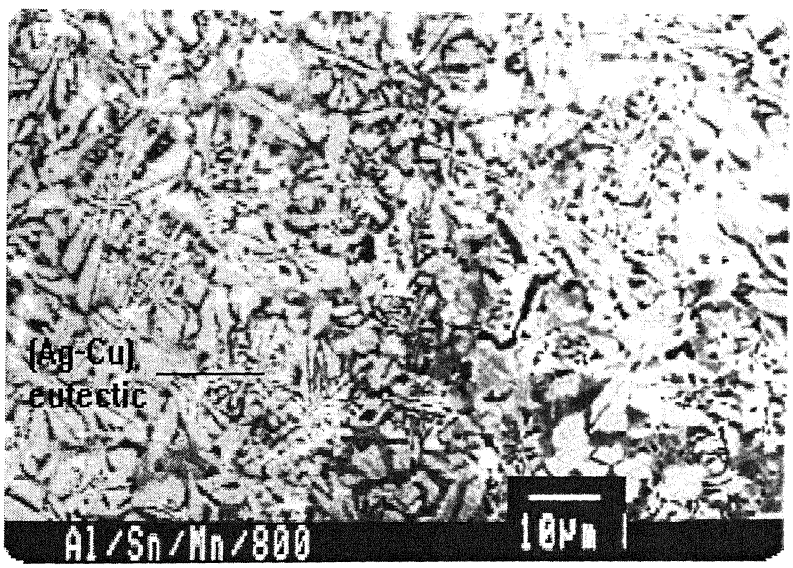

Figure [27a]: Photomicrograph of the Al_2O_3/Ti/60Ag-30Cu-10Sn/Mn System showing the four-phase structure which includes the (Ag-Cu) eutectic.

The photomicrograph of Figs. 27 a and b, show lamellar structure of the eutectic Ag-Cu, bright matrix of proeutectic (Ag), dark gray particles of Ag-Mn solid solution and the dark small particles are assumed to correspond to that of TiCu intermetallics as observed in the other systems. The composition of the above, four-phase structure obtained

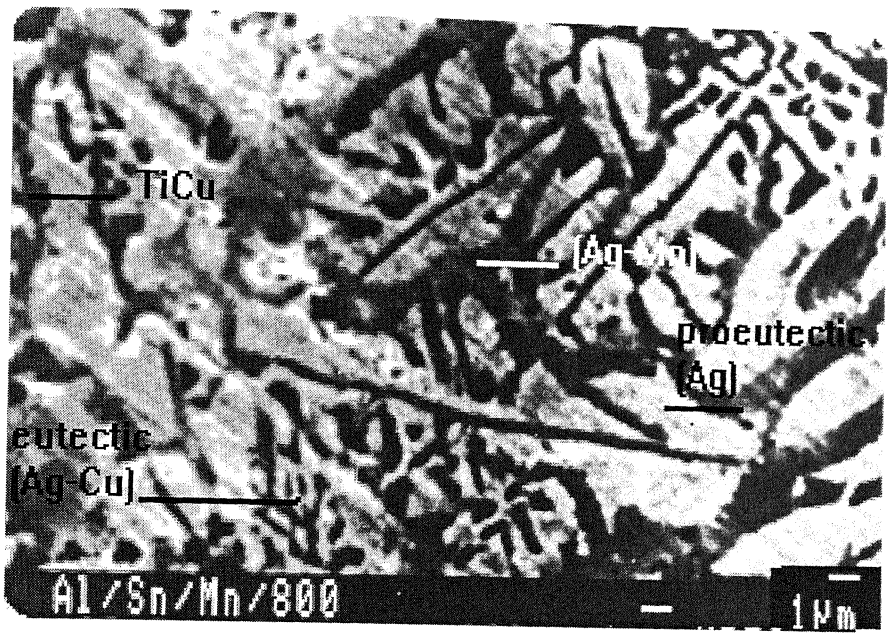

Figure [27b]: Photomicrograph of the Al_2O_3/Ti/60Ag-30Cu-10Sn/Mn System showing the four phase structure which includes the (Ag-Cu) eutectic dark gray (Ag-Mn) gray proeutectic (Ag) and dark particles of TiCu.

from EPMA is 36.61 at. pct. Ag, 29.35 at. pct. Cu, 29.23 at. pct. Mn and 4.8035 at. pct. Sn. It was not possible to analyze individual phase because of the fine structure. The lamellar structure is assumed to be the Ag-Cu eutectic and it has formed by the eutectic reaction occurring at 779^0C at 40 at. pct. Cu balance Ag [16], Fig 27b. The Ag-Mn phase diagram shows that there is a solid solution of (Ag) and (αMn) up to a temperature of 711^0C and a solid solution of (Ag) with Mn at 800^0C [34]. The large dark particles are those of the TiCu intermetallic.

3.9 Binary Phase Diagrams (Ni-Ti & Ni-Cu)

The Figure 28 shows the Ni-Ti phase diagram. The phase diagram shows that there are several binary intermetallics of Ni-Ti, namely Ni_3Ti, NiTi, $NiTi_2$ etc.

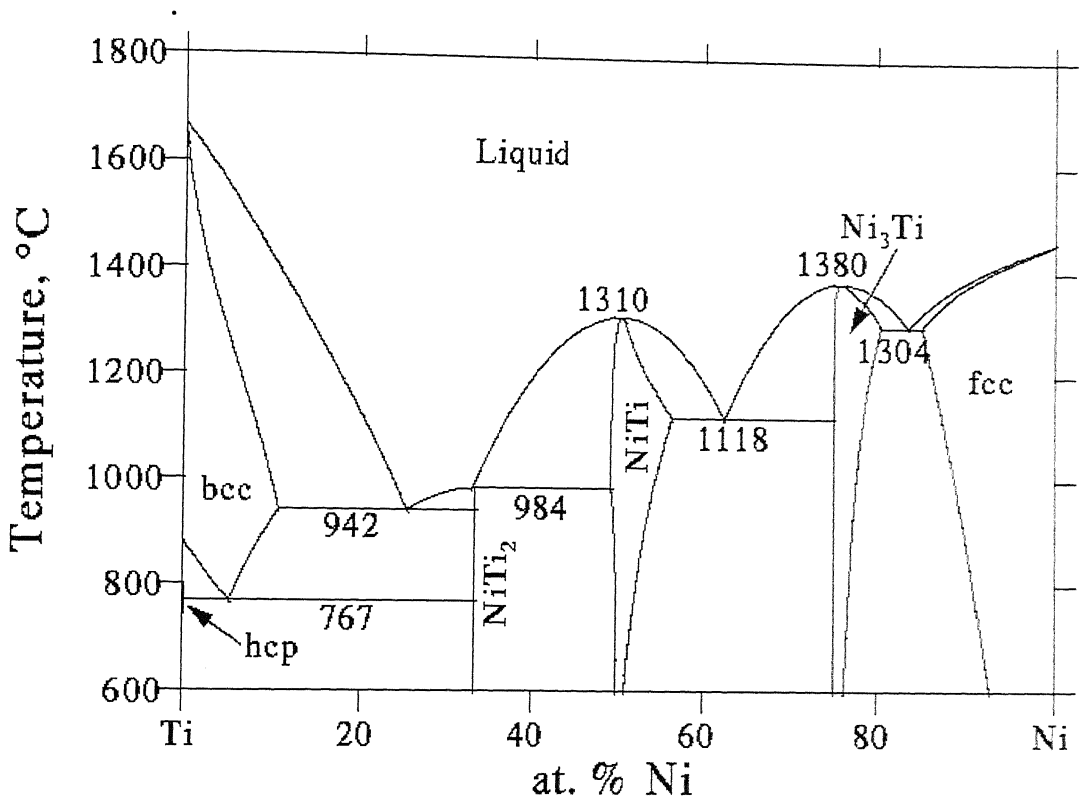

Figure 28: The Ni-Ti phase diagram

We have observed from the EPMA study, shown in Table-3, that there was formation of $Ni(Cu)Ti_2$, $Ni_3(Cu)Ti$ intermetallics in the Al_2O_3/Ti/60Ag-30Cu-10Sn/ Ni system. The dark particles, in the middle of the filler metal region as shown in Figs. 9 and 10, are $Ni_3(Cu)Ti$. The analysis of the dark particles has shown 1.64 at. pct. Cu, 69.97 at. pct. Ni and 28.65 at. pct. Ti with small amounts of Ag, Al and Sn for this phase. The metal Cu substitutes for Ni in this phase. The Ni_3Ti phase has been reported [22], with a composition of 75 at. pct. Ni balance Ti. As seen in Fig. 28 we see the Ni concentration in this intermetallic is around 75 at. pct. The Ti concentration in this phase is observed to be higher than reported [22] and seen in Fig.28.

The $Ti_2Ni(Cu)$ compound forms as light gray irregular structure, Fig.11 near the Ti/filler-metal interface. The Ti_2Ni intermetallic has been reported to form by the following eutectic reaction at 942^0C. $L \longrightarrow (\beta Ti) + Ti_2Ni$. Experimentally we have obtained 24.94 to 25.94 at. pct. Ni, 5.62 to 6.29 at. pct. Cu and 67.9 to 68.22 at. pct. Ti with very small amounts of Al and Sn. Assuming that Cu substitutes for Ni in the Ti_2Ni phase the effective Ni concentration has a range of 30.74 to 31.56 at. pct. , which is close to the desired 33.33 at. pct. Ni for this intermetallic compound [22], as seen in the Fig.28.

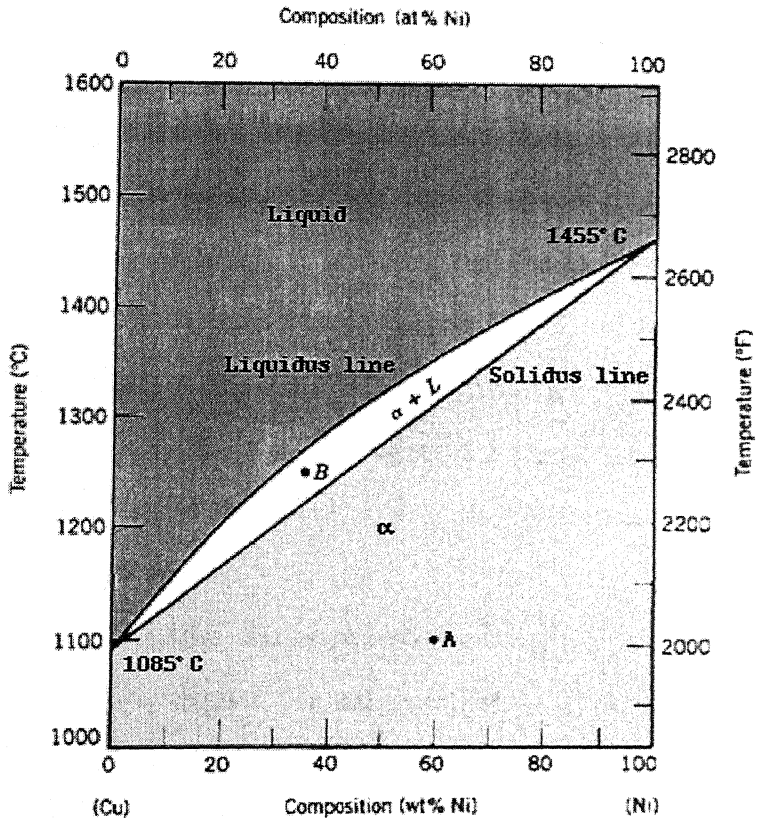

Figure 29: The Ni-Cu phase diagram

The Ni-Cu phase diagram, Fig.29 shows that below 1085^0C we have solid solution of Ni-Cu and this explains the substitution of Ni by Cu in $Ni(Cu)Ti_2$ and $Ni_3(Cu)Ti$.

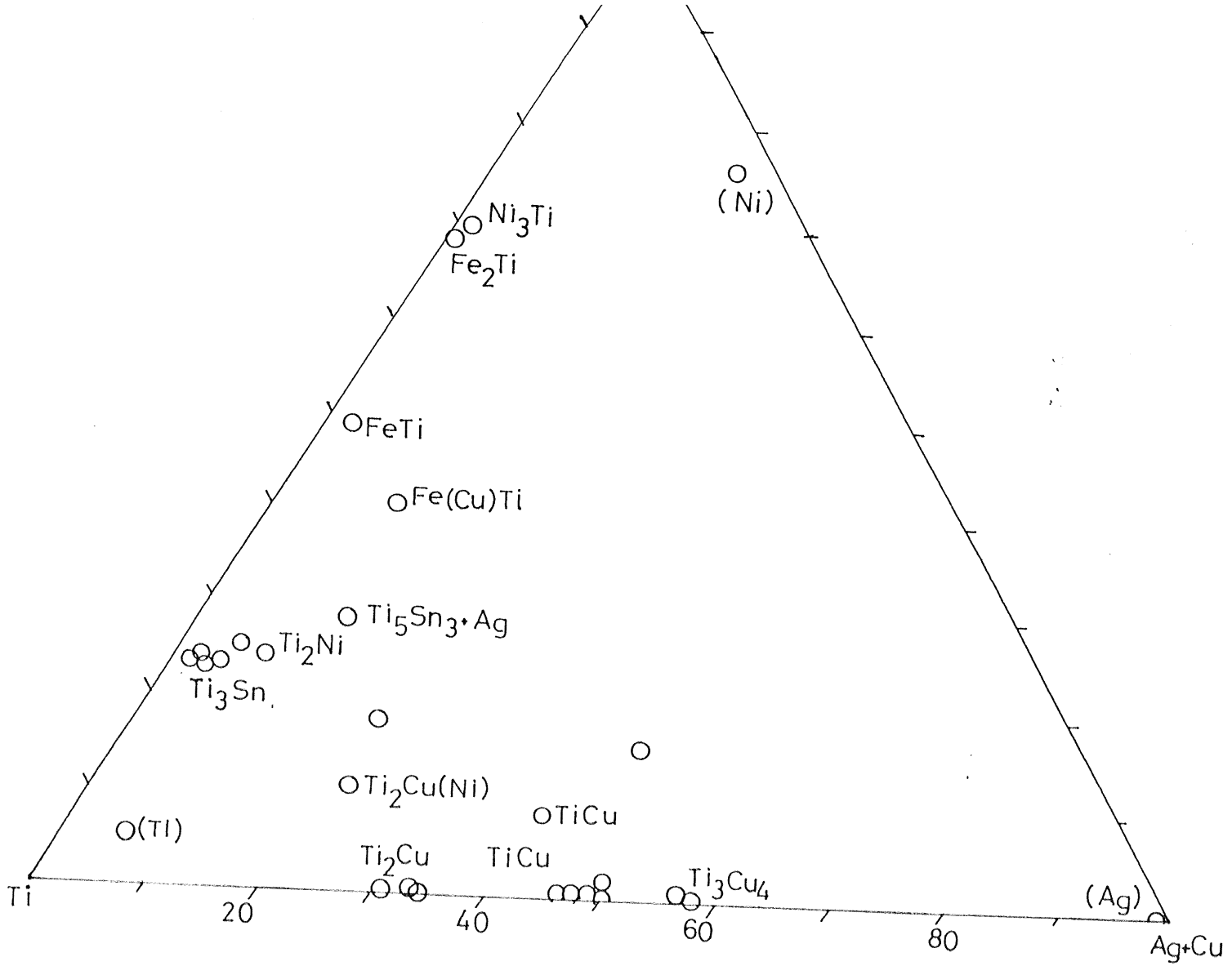
Ni3Ti
Fe2Ti
(Ni)
FeTi
Fe(Cu)Ti
Ti5Sn3·Ag
Ti2Ni
Ti3Sn
Ti2Cu(Ni)
TiCu
(Tl)
Ti2Cu
TiCu
Ti3Cu4
(Ag)
Ti
20
40
60
80
Ag+Cu

Fig.30.

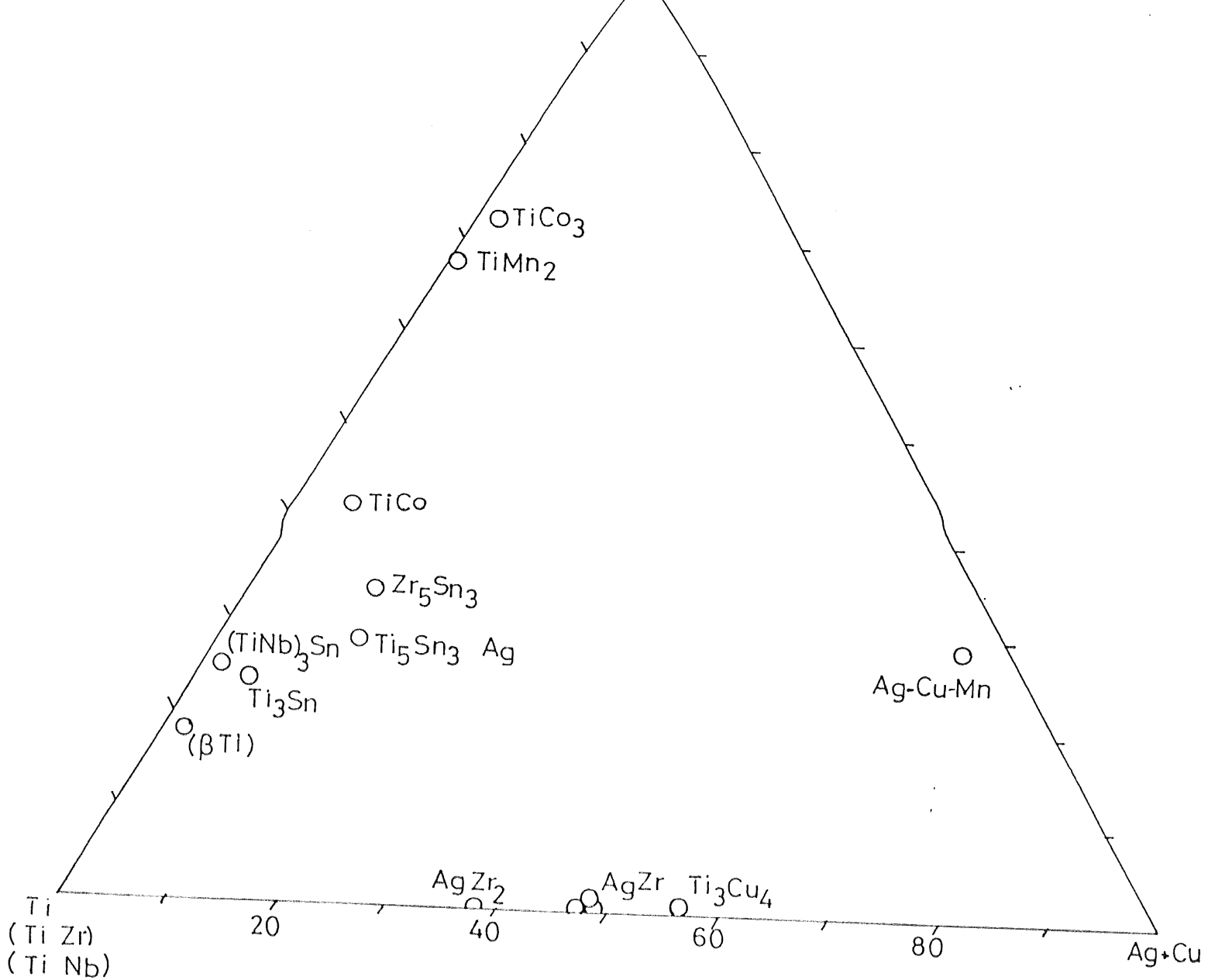
TiCo3
TiMn2
TiCo
Zr5Sn3
(TiNb)3Sn
Ti5Sn3
Ag
Ti3Sn
(βTi)
Ag-Cu-Mn
AgZr2
AgZr
Ti3Cu4
Ti
(Ti Zr)
(Ti Nb)
20
40
60
80
Ag+Cu

The Fe_2Ti intermetallic is observed with approximately 32 at. pct. Ti and 68 at. pct. Fe.

The Ni_3Ti intermetallic has been observed with 28.65 at.pct Ti and 69.67 at.pct. Ni. There has been approximately 2 at. pct. solubility of the other elements in this intermetallic. The Ti_2Ni intermetallic has been observed with 68 at. pct. Ti and 26 at. pct. Ni. There has been a solubility of approximately 6 at. pct. Cu in the Ni_3Ti phase. The Ni solid solution has been observed with 17.91 at. pct Cu soluble in it.

The TiAg intermetallic has been observed with 42 at. pct. Ti and 58 at. pct. Ag.There has been a solubility of metal Cu in this intermetallic.

The $TiCo_3$ intermetallic has been observed with 25.97 at. pct. Ti and 72 at. pct. Co. There has been a solubility of 2 at. pct. of Cu in this intermetallic. The TiCo intermetallic has been observed with 53.5 at. pct. Ti and 41 at. pct. Co. There has been a solubility of 5 at. pct. of Cu and small amounts of other elements in this intermetallic.

The $AgZr_2$ intermetallic has been observed with approximately 53 at. pct. Zr and 26 at. pct. Ag. The metal Cu substitutes Ag by approximately 7 at.pct. and Ti substitutes Zr by 13 at. pct. The AgZr intermetallic has been observed with approximately 31 at. pct. Zr and 45 at. pct. Ag. The metal Cu substitutes Ag by approximately 4 at.pct. and Ti substitutes Zr by 17 at. pct. The Zr_5Sn_3 intermetallic has been observed with approximately 53 at. pct. Zr and 33.57 at. pct Sn. There has been solubility by small amounts of Ti, Ag and Cu.

The $TiMn_2$ intermetallic has been observed with 31.7 at. pct. Mn and approximately 68 at. pct. Ti. A eutectic of Ag-Cu-Mn has been observed with composition such as 55.8 at. pct. Ag , 23 at. pct. Mn and 18 at. pct. Cu.

The intermetallic $(TiNb)_3Sn$ has bben observed with 57 at. pct. Ti , 16 at. pct. Nb and 25 at. pct. Sn.

Conclusion:

- Important intermetallic phases observed in different systems are summarized as follows:

Metallic Substrate	Iron	Nickel	Zirconium	Niobium
Intermetallic phases	FeTi, Fe_2Ti, Ag-Cu eutectic, TiCu, Ti_2Cu, Ti_3Sn, Ti_5Sn_3, (Ag), Fe(Cu)Ti.	$Ti_2Ni(Cu)$, $Cu_3(Ni)Ti_2$, $Ni_3(Cu)Ti$, $Ti_2Cu(Ni)$, (Ni-Cu), (Ag), Ti_3Sn, TiCu.	Zr, $Ag(Cu)Zr_2(Ti)$, $AgZr_2$, Zr_5Sn_3, (Ti-Zr), Ag(Cu)Zr(Ti), (Ag).	(Ti-Nb), $(TiNb)_3Sn$, (Ag), Ti_5Sn_3, (Cu)+(Ag-Cu), Ti_3Cu_4, Ti_3Sn, TiCu.

Metallic Substrate	Cobalt	Chromium	Tantalum	Manganese
Intermetallic phases	(Ag-Cu), TiCo, TiCo(Cu), Ti_5Sn_3, $TiCo_3$, (Ag), Ti_3Sn, TiCu.	(Ti-Cr), $\gamma CuTi$ + $\gamma AgTi$, TiCu(Ag), $Ti_2Cu(Ag)$, Ti_5Cu_3Cr, Ti_3Sn, (Ag).	(Ti), TiCu, Ti_2Cu, Ti_3Sn, (Ag),	(βTi), $TiMn_2$, (Mn), Ag-Cu eutectic, Ag-Mn Solid Solution.

- The microstructure of the phases formed at different positions of the diffusion couple is characterized.
- A number of intermetallics of Ti and Cu have been observed. These are; Ti_2Cu, TiCu, Ti_3Cu_4, Ti_2Cu_3. In most cases, the intermetallics have some solubility for elements like Ag, Al, Fe, Ni , Sn, Nb etc.
- Eutectic of Ag-Cu has been observed as a lamellar structure in the Al_2O_3/Mn, Al_2O_3/Fe, Al_2O_3/Nb and Al_2O_3/Cr systems.

- Two binary intermetallics of Sn and Ti have been observed, namely, Ti_3Sn, and Ti_5Sn_3. There has been some solubility of Cu in these phases.
- Two binary intermetallics FeTi and Fe_2Ti of the Fe-Ti system have been observed in alumina bonded with Fe. Cu has been observed to substitute for Fe in FeTi.
- One unknown ternary intermetallic of Ti-Cu-Fe has been observed in alumina bonded with Fe.
- Two binary intermetallics of Ni and Ti have been observed in alumina bonded with Ni. These are Ni_3Ti and $NiTi_2$. The metal Cu substitutes for Ni in Ni_3Ti and $NiTi_2$.
- One binary intermetallic of Zr and Sn i.e. Zr_5Sn_3 has been observed in alumina bonded with Zr.
- $AgZr_2$ and AgZr intermetallics were formed near the upper part of the diffusion couple and Ti has been observed to substitutes for Zr in both the intermetallics.
- Solid solution of Ti-Nb has been observed at the Nb/filler –metal interface in alumina bonded with Nb. No intermetallic of Nb with other elements has been observed.
- Two binary intermetallics $TiCo_3$ and TiCo of the Co-Ti system have been observed in the major parts of the diffusion couple, when alumina was bonded with Co. The metal Cu substitute for Co in both the intermetallics.
- Solid solution of Cr-Ti form at the Cr filler metal interface in a diffusion couple of alumina bonded with Cr.
- A ternary phase of Ti-Cu-Cr, Ti_5Cu_3Cr, has been observed at the upper part of the diffusion couple.
- No intermetallic of Ta has been observed in alumina-Ta diffusion couple. Ta has a melting point of 3020^0C, which is very high as compared to 800^0C, the temperature at which the experiment was carried out. The diffusion of Ta

was expected to be slow when compared to other elements at the brazing temperature.

- One binary intermetallic of Ti and Mn i.e $TiMn_2$ was formed at the Mn/filler-metal interface in alumina bonded with Mn. It has been observed that there was an extensive diffusion of Ti in this system, and (Ti) is formed at the Mn/filler-metal interface. This behavior was also observed in the alumina-Ta diffusion couple.
- It has been observed that for proper bond formation prior to vacuum brazing polishing and cleaning of the surfaces of the filler-metal, active-metal, base metal and ceramic is essential.
- Alignment and close fitting of all the components i.e. filler-metal, active-metal, base metal and ceramic is essential for ceramic-base metal bonding.
- The heating rate of the diffusion couple has to be limited to prevent alumina ceramic from cracking.

REFERENCES:

(1) Nicholes M. G., Materials aspect of ceramic to ceramic and ceramic to metal bonding, Harwell Lab., IIW, Madrid, Spain, Sept.1992.

(2) Santella M.L., High Strength silicon nitride brazed joints, ORNL, TN, 22nd AWS International Brazing & Soldering Conf., Paper B3C, Detroit, MI, Apr. 16-18 1991.

(3) Xu R., Indacochea J.E., Brazing silicon nitride to metals using active filler metal, Univ. of ILL., Paper B2A , 23rd AWS International Brazing & Soldering Conf., Chicago, IL, Mar. 24-26, 1992.

(4) Dunkerton S., Brazing sialon to steel for automotive application, TWI, Abington, UK. , Paper B2E, ibid.

(5) Lee H. -K., Lee J. –Y, Decomposition and interfacial reaction in brazing of silicon carbide by copper based active alloys, J. Mater. Sci. Lett., 11, pp.550-53, 1992.

(6) Santella M.L. , Pak J.J. , Fruehan R.J. , Analysis of microstructures formed by brazing Al_2O_3 & ZrO_2 with Ag-Cu-Ti alloys, ORNL,TN,Paper B1C, 20th AWS International Brazing &Soldering Conf. , Wash. D.C. , Apr.3-5,1989.

(7) Mizuhara H., Huebel E., Joining ceramic to metal with ductile active filler metal, Welding journal 65[10], Oct., pp.43-51, 1986.

(8) Giles Hampston and David M.Jacobson, Principals of soldering & brazing, ASM International [The Materials Information Society], 1993.

(9) Feduska, w., High-temperature brazing alloy-base metal wetting reaction Weld. J. Vol. 38[3], Mar., 122-30.

(10) J.F. Lancaster, Metallurgy of Welding Soldering & Brazing, 126-127, 1965.

(11) M. Schawartz, Brazing: For the engineering technologist, Chapman and Hall, 1995.

(12) H. Mizuhara and T.Oyama, ceramic/ metal seals, Reprinted from ASM Hand book, Vol-4; ceramic and glass, 1993.

(13) Brazing HandBook, American Welding Society, Fourth Edition, AWS Committee on Soldering & Brazing, 1991.

(14) G Sheward, High Temperature Brazing in Controlled Atmospheres UKAEA, Springfields Laboratories, Preton, UK, 35-36, 1989.

(15) The Phase Diagram Web, A free service of The Georgia Tech. Joint Student Chapter of ASM/TMS.

(16) J.L. Murray, Binary Alloy Phase diagrams, T.B. Massalski, editor, ASM Int., Materials Park, Ohio, Vol. 2, pp 1117-1118, 1989.

(17) A.Hellawell and W. Hume-Rothery, Philos-Trans-Roy. Soc., London, 249,417-459[1957].

(18) J.L. Murray, Binary Alloy Phase diagrams, T.B. Massalski, editor, ASM Int., Materials Park, Ohio, Vol. 1, pp 9, 1989.

(19) J.L. Murray, Binary Alloy Phase diagrams, T.B. Massalski, editor, ASM Int., Materials Park, Ohio, Vol. 2, pp 2076,2079,1989.

(20) J.L. Murray, Binary Alloy phase diagrams, T.B. Massalski, editor, ASM Int., Materials Park, Ohio, Vol. 1, pp 970-972,1989.

(21) M.Hansen and K. Anderko, Constitution of Binary Alloys, McGraw-Hill, NewYork,J.L. Murray, Binary Alloy Phase diagrams, T.B. Massalski, editor,ASM Int., Materials Park, Ohio, Vol. 1, pp 970-972,1989.

(22) J.L. Murray, Binary Alloy Phase diagrams, T.B. Massalski, editor, ASM Int., Materials Park, Ohio, Vol. 2, pp 1763-1769,1989.

(23) C. B. Alcock, K.T. Jacob, S.Zador, O.Von Goldbeck, H.Noworty, and K.Seifert, Physico-Cemical properties of its compounds and Alloys, O.

Kubaschewski, Ed., Atomic Energy Review Special Issue No.6, International Atomic Energy Agency, Vienna [1976], J.L. Murray, Binary Alloy Phase diagrams, T. B. Massalski, editor, ASM Int., Materials Park, Ohio, Vol. 1, pp. 87-88,1989.

(24) J.P. Abriata, J.C. Bolcich, and D. Arias; Bull. Alloy Phase diagrams, 4[2], Sep 1983, J.L. Murray, Binary Alloy Phase diagrams, T. B. Massalski, editor, ASM Int., Materials Park, Ohio, Vol. 2, pp. 2087-2089,1989.

(25) J.L. Murray, Binary Alloy Phase diagrams, T. B. Massalski, editor, ASM Int., Materials Park, Ohio, Vol. 2, pp. 2142-2143,1989.

(26) J.L. Murray, Binary Alloy Phase diagrams, T. B. Massalski, editor, ASM Int., Materials Park, Ohio, Vol. 2, pp. 1699-1703,1989.

(27) J.L. Murray, Binary Alloy Phase diagrams, T. B. Massalski, editor, ASM Int., Materials Park, Ohio, Vol. 1, pp. 803-809,1989.

(28) T. Nishizawa and K. Ishida, [1984], Binary alloy Phase diagrams, ASM Int., Materials Park, Ohio, Vol. 1, pp. 970-972,1989.

(29) J.L. Murray, Binary Alloy Phase diagrams, T. B. Massalski, editor, ASM Int., Materials Park, Ohio, Vol. 1, pp. 873-874,1989.

(30) J.L. Murray and K.J. Bhansali, Binary Alloy Phase diagrams, T. B. Massalski, editor, ASM Int., Materials Park, Ohio, Vol. 1, pp. 74-78,1989.

(31) J.L. Murray, Binary Alloy Phase diagrams, T. B. Massalski, editor, ASM Int., Materials Park, Ohio, Vol. 2, pp 2099-2100,1989.

(32) J.L. Murray, Binary Alloy Phase diagrams, T. B. Massalski, editor, ASM Int., Materials Park, Ohio, Vol. 2, pp 1592-1599,1989.

(33) Y. Saleh and H. Margolin, Acta metall., 27,535-544,1979.

(34) M. Hansen and K. Anderko, Constitution of Binary Alloys, McGraw-Hill, New York, J.L. Murray, Binary Alloy Phase diagrams, T. B. Massalski, editor, ASM Int., Materials Park, Ohio, Vol. 1, pp 43,1989.

(35) T. M. Valentine, M.G. Nicholus and M. J. Waite, "The wetting of alumina by copper alloyed with titanium and other elements " J. Mat. Sc. Vol.15, No. 7-9, pp.2197-2206, 1980.

(36) M. G. Nicholus, "Ceramic metal interfaces", Surface and Interface of ceramic material, Series E, Applied science Vol.173, Kluwer Acedemic Publisher London, pp. 393-417, 1989.

(37) M. Samandi, M. Gudze and P. Evans "Application of ion implantation to ceramic/metal joining", Nuclear Instrument and Method in Physics Research, Section B, Beam Interaction with Materials and Atoms, Vol. 127-128, pp. 669-672, May 2, 1997.

(38) R. Loheman et al, "Bonding mechanism in silicon nitride brazing", J. Am. Cer. Soc., Vol. 73,No.3, pp. 552-558, 1990.

(39) S. D. Peteves et al," Reactive route to ceramic joining; Fabrication, interfacial chemistry and joint properties", Acta Materialia, V 46, No.7, Apr.10 pp.2407-2414, 1998.

(40) W. Tillman et al, "Heat resistant active brazing of sillcon nitride, Part2: Metallurgical characterization of the braze joints", Welding Journal, March, pp. 103-109, 1998.

(41) N.D. Tinsley, J. Huddleston and M.R. Lacey, Materials and Manufacturing Process V13, n4, July, pp. 491-504, 1998.

(42) M. L. Santella and J. J. Pak "Brazing titanium vapor coated zirconia", Weld. J., Vol.72, No.4, pp.165-172, 1993.

(43) Hongqi Hao et al "Joining of ZrO_2 ceramic to stainless steel and to itself using $Ag_{57}Cu_{38}Ti_5$ filler metal" J. Am. Cer. Soc., 78[8], pp.2157-2160, 1995.

(44) H.K. Lee and J.Y. Lee, "Decomposition and interfacial reaction in brazing of SiC by Copper based active alloy", J. Mater. Sc. Vol.11, pp. 550-552, 1992.

(45) C.Iwamoto and S.I.Tanaka, "Reactive wetting of Ag-Cu-Ti on SiC in H.R.T.M." Acta. Matre. Vol. 46, No.7, pp. 2381-2386, 1998